Introduction *3*
Methods *5*
Results *7*
Lattice degeneration **9**
Retinal Cystic Tuft **11**
Peripheral Retinal Hole **13**
Snail track degeneration **17**
White Without Pressure **17**
Peripheral retinoschisis **18**
Retinal tear **22**
Retinal dialysis **23**
Case series **24**
Discussion *33*
Conclusion *41*
References *42*

Introduction

Since its introduction in 1991, Optical Coherence Tomography (OCT) proved to be a fundamental tool for the diagnosis and management of various macular diseases. It currently represents a necessary instrument in the ophthalmological clinical practice for the diagnosis and monitoring of different macular disorders, as age related macular degeneration, choroidal neovascularization, vitreo-macular interface pathologies, macular edema, genetic disorders and many others[12].
Although conventional OCT devices are able to perform an imaging in a limited central part of retina, recently wide field and ultra-wide field imaging devices have been introduced, allowing to image the retina up to 50° and to 200° of the retina, respectively, and nowadays the imaging of retinal periphery has gained importance in the characterization and management of various vitreo-retinal diseases as diabetic retinopathy, retinoschisis, retinal detachment and peripheral degenerations, among many others[3,4,5,6,7,8,9]. The ongoing development of ultra-wide field-OCT, with its ability to capture retinal structures to the far periphery, including the anterior edge of the vortex vein ampulla and beyond to pars plana has attracted vitreoretinal experts to understand the pathology and structural abnormalities behind peripheral retinal lesions with increased accuracy[4]. Indeed, the characterization of specific peripheral retinal areas with ultra-wide field OCT imaging may provide insights that directly affect clinical management decisions, as monitoring retinal detachment associated with retinoschisis, or differentiating them, by more directly observing the retinal layers[10]. Also, wide field OCT has been employed in analyzing specific structural features of peripheral vitreo-retinal interface and retinal lesions, such as vitreoretinal attachment and traction, full-thickness hole or tear, and sub-retinal fluid and the association with retinal detachment, and it has been suggested that it may improve the understanding of pathophysiology and risks of retinal detachment[9,10]. However, there is still a limited existing literature evaluating peripheral retinal degenerations and rhegmatogenous lesions by means of ultra-wide field OCT.
Currently prophylactic treatment of retinal degenerations with either laser or cryotherapy is controversial and not well defined by clinical recommendations[11]. The evidence available suggests that most of the peripheral retinal degenerations should not be treated except in high-risk situations, and well-designed, prospective, randomized clinical studies to clarify the benefit-risk ratio of prophylactic treatment are still lacking[12]. In addition, there is still a lack of reference nomenclature for peripheral retinal lesions.
For all these reasons the study of peripheral retina with new widefield and ultra-wide field imaging modalities, including OCT, is a research field with growing interest.
Therefore, we conducted the present study with the aim to characterize peripheral degenerations and rhegmatogenous retinal lesions, by means of Optos Silverstone (Optos PLC; Dunfermline, UK), a new multimodal imaging platform which allows the acquisition of swept-source OCT (SS-OCT) scans of the extreme retinal periphery. We studied the principal findings of peripheral retinal degenerations, as the vitreoretinal interface over the lesions, the presence of associated full-thickness retinal defects or sub-retinal fluid, not always evident on clinical examination. We also employed ultra-wide field OCT to systematically analyze peripheral retinal

rhegmatogenous degenerations, as retinal tears, retinal holes, retinal dialysis and their relationship to the vitreous body. Moreover, we reported a case series in which the employment of peripheral SS-OCT supported or influenced the clinical decision.

Methods

We performed a retrospective observational study, on 95 patients previously diagnosed with peripheral retinal degenerations and/or rhegmatogenous lesions, referred to the Eye Clinic, Careggi University Hospital, in Florence (Italy) between October 2022 and October 2024. The study conformed to declarations of Helsinki and informed consent was obtained from all the patients.

The patients who were found to have peripheral retinal degenerations or rhegmatogenous lesions as seen on indirect ophthalmoscopy, above the age of 18 years, were included in the study. Patients with medium opacities, or not collaborating behavior, impeding a proper imaging acquisition were excluded from the study.

Each patient underwent a complete ophthalmological examination with measurement of best corrected visual acuity (BCVA), slit-lamp biomicroscopy, dilated fundus examination with a Volk digital wide field lens, and multimodal imaging assessment including peripheral SS-OCT (Optos Silverstone) (Optos PLC; Dunfermline, UK).

Optos Silverstone SS-OCT is a new multimodal imaging platform with allows the acquisition of SS-OCT scans of the extreme periphery. It produces an initial high-resolution scanning laser ophthalmoscope (SLO) fundus image up to 200° and then uses navigated SS-OCT line or volume scans of the far retinal periphery as mapped by ultra-wide field SLO images. A signal source of 1050 nm wavelength, axial resolution of < 7 microns, and transverse resolution of < 20 microns provide deeper tissue penetration for clear, detailed imaging of the retina from the vitreous through the choroidal-scleral interface, in less than half a second with a single click. Line scans with widths of 6 mm, 14 mm, and 23 mm and volume scans with height ranging from 3 mm to 9 mm, and width from 6 mm to 14 mm can be produced using optomap-guided ultra-wide field OCT.

SS-OCT imaging was performed by two experienced ophthalmologists, expert in retinal imaging acquisition (DB, CN). At baseline, color optomap images, ultra- wide field 6 mm line and 6 mm volume OCT scans were obtained from all patients. Ultra-wide field 6 mm HD volume and 23 mm extended line OCT and green autofluorescence scans were also captured, at the photographer's discretion. Each patient images were assessed on several specific areas of interest by 2 physicians (DB, CN), which included confirmation of the diagnosis, pathology location and the quality of the images acquired. Each peripheral retinal degeneration was distinguished according to different parameters. Depending on the pathology location, each alteration was classified as mid-peripheral or far peripheral based on the classifications and guidelines for wide field imaging from the International Wide Field Imaging Study Group[4]. As previously published, the mid-periphery is the region of retina extending from the vascular arcades to the posterior edge of the vortex vein ampulla and the far periphery is the part of retina anterior to the vortex vein ampulla.

We collected the main demographic data of the patients studied, as age and sex, and the main clinical characteristics of the eyes analyzed, as average refractive error, BCVA, lens status. We also collected data regarding the symptoms referred. Then we analyzed the principal ultra-wide field optomap and SS-OCT retinal findings associated with peripheral degenerations and the vitreoretinal interface at the level of the lesions, as the presence of full thickness associated alterations, subretinal fluid, vitreoretinal traction and other characteristics. We reported OCT characterization of rhegmatogenous retinal lesions, as retinal tears and holes, evaluating the presence of vitreous traction, subretinal fluid, the morphology of the edges in retinal holes and other features. We evaluated also the retinal lesions localization, and the presence of vitreous detachment, analyzed by examination of fundus photography or OCT scan. Finally, we reported a case series, in which peripheral OCT findings had an influence on clinical management.

Results

In this study 107 eyes of 95 patients with peripheral retinal degenerations and/or rhegmatogenous lesions were scanned with the Optos Silverstone platform.
The mean age of the population in this study was 50.9 (standard deviation ±15). Forty-six men and 49 women were included in the study. The mean refraction (Spherical Equivalent) was −2.18 diopters (SD, ±2.5 diopters), ranging from -7.50 to 0. The median LogMar BCVA was 0.0, the average BCVA was 0.03 (standard deviation ±0.11). Ninety-one patients were phakic, 4 patients were pseudophakic.
The baseline demographics of the study population are resumed in Table 1.

Table 1. Baseline demographics and clinical characteristics of patients included in the study.

Total patient number	95
Total eyes number	107
Age (years, mean ± SD)	50.9 ± 15
Gender (M/F)	46/49
Average refractive error (diopters; mean ± SD)	−2.18 ± 2.5
Median LogMar BCVA	0.0
Lens Status (phakia/pseudophakia)	91/4

BCVA = best corrected visual acuity; F = female; M = male; SD = standard deviation.

A total of 130 lesions were imaged, 12 different types of peripheral lesions were identified (Table 2). High quality images of the peripheral retina and vitreoretinal interface were obtained in all the lesions.
The most prevalent peripheral lesions observed were retinal tears (34 cases) and lattice degenerations (25 cases). The other commonly observed lesions were retinal holes (21), peripheral retinoschisis (17) and retinal tufts (11). Less common lesions were schisis/detachment (7 cases), snail track degeneration (4 cases), white without pressure (4 cases) microcystic degeneration (2 cases), dialysis (2 cases), condensed vitreous (2 cases), paving stone degeneration (1 case). Forty-five degenerations were mid-peripheral and 85 were peripheral. In 18 cases the lesions were in highly myopic eyes (myopia >6 diopters). Six lesions were in eyes with previous history of trauma. In forty cases the lesion was associated to myodesopsya, 34 lesions were associated to phosphenes reported by the patients.

Table 2. Different types of peripheral retinal degenerations imaged with Optos Silverstone.

Type of retinal degeneration	Number
Retinal tear	34
Lattice degeneration	25
Retinal hole	21
Peripheral Retinoschisis	17
Retinal tuft	11
Schisis/Detachment	7
Snail track degeneration	4
White without pressure	4
Dyalisis	2
Condensed vitreous	2
Microcystic degeneration	2
Paving stone degeneration	1

The detailed ultra-wide field SS-OCT findings of the most common peripheral retinal lesions are described in the paragraphs below.

Figures legend
OCT= Optical Coherence Tomography
SS-OCT=Swept Source-Optical Coherence Tomography
UWF= Ultra-Wide Field

Lattice degeneration

We analyzed 25 cases of lattice degeneration, successfully imaged using ultra-wide field SS-OCT with the Optos Silverstone platform.

On ultra-wide field color fundus imaging, the lesions appeared as elongated, whitish, peripheral alterations, typically parallel to the ora serrata, with attenuated underlying blood vessels passing through the lattice lesions. Twelve lesions had a focal shape, while 13 displayed a linear configuration. Ultra-wide field SS-OCT showed irregular thinning of the neuroepithelium in all cases. Full thickness retinal holes (Fig 1A) were observed in 21 cases, while retinal tears (Fig 1C) were present in 2 cases, with subretinal fluid identified in 4 cases. Additionally, OCT detected microcystic changes in the perilesional retina in 4 cases. Peripheral OCT also provided valuable insights regarding the vitreoretinal interface, showing vitreous liquefaction over the lattice lesions in 19 cases. Vitreoretinal traction was observed in 22 cases, focal in 9 cases (Fig. 1A) and diffuse in 13 cases (Fig. 1B). In 3 cases, hyperreflective deposits were observed within the retina, while irregularities of the pigmented epithelium were present in 20 cases. Choroidal thinning was detected in 19 cases (Fig. 1C). Posterior vitreous detachment was noticed in 8 cases.

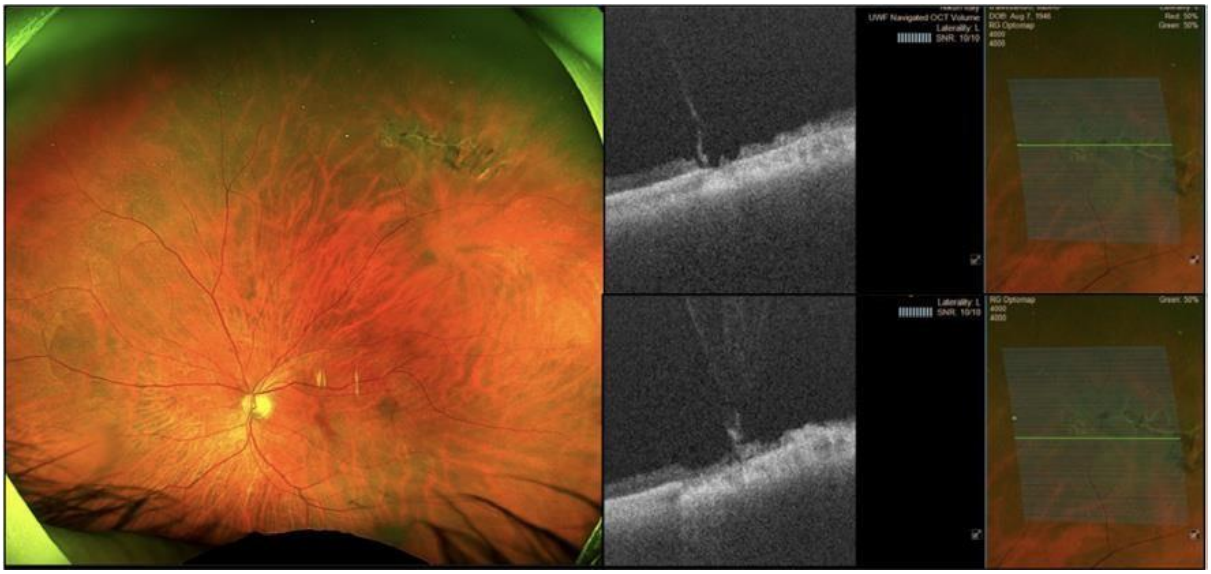

Fig. 1A. UWF SS-OCT findings in lattice degeneration. Irregular thinning of the neuroepithelium, full thickness retinal holes, overlying vitreous liquefaction and firm vitreo retinal adhesions at the edge of the degeneration are depicted.

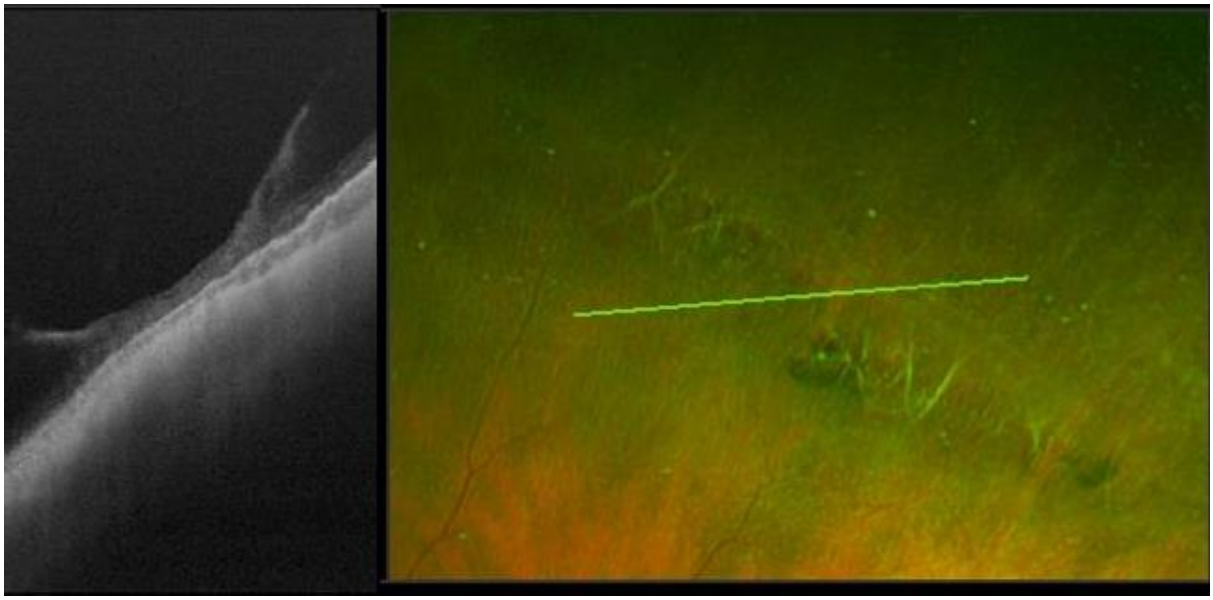

Fig. 1B. UWF SS-OCT findings in lattice degeneration. Diffuse vitreous traction over lattice degeneration and choroid thinning are visible.

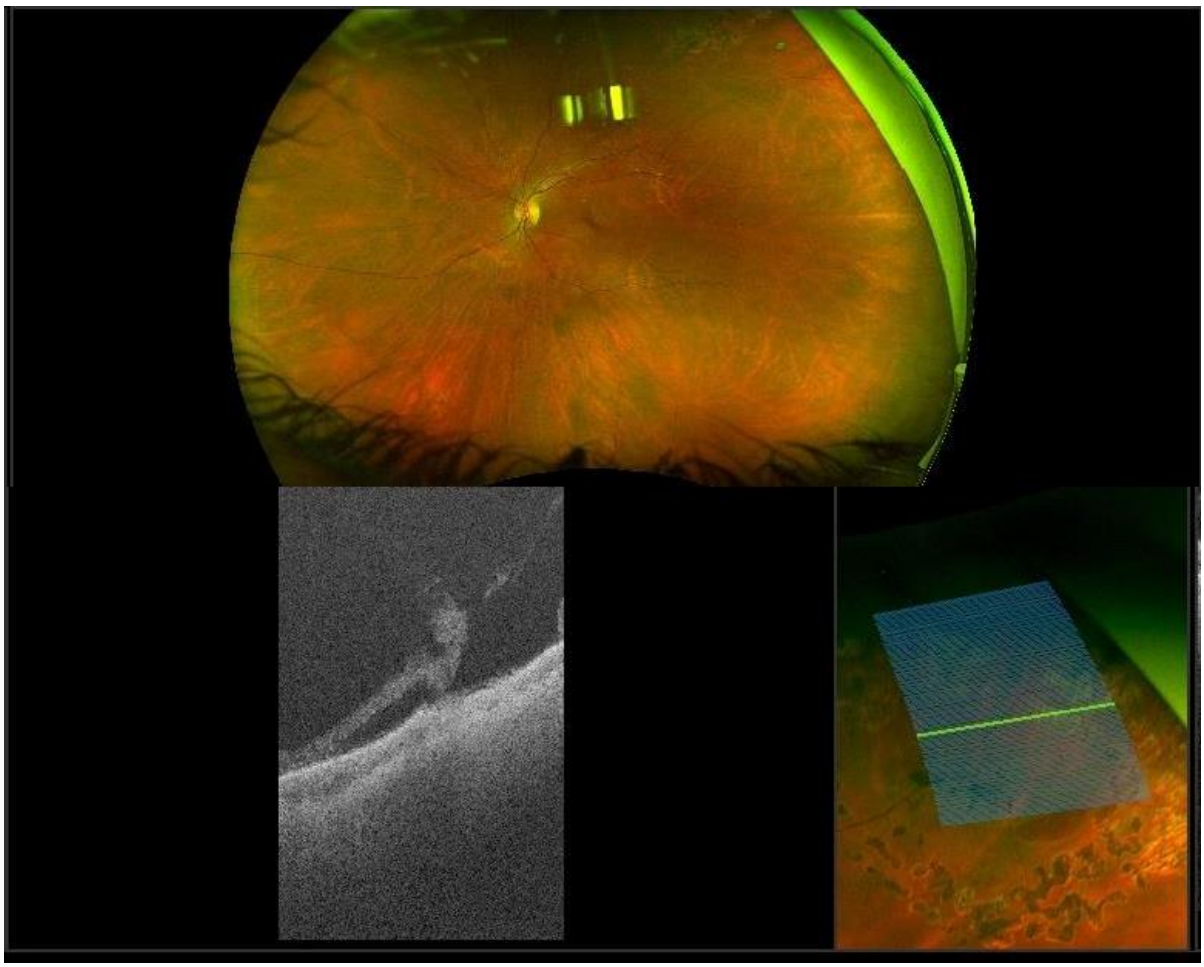

Fig 1C. UWF SS-OCT findings of a retinal tear on lattice degeneration, previously treated with laser. Vitreous traction and subretinal fluid are visible.

Retinal Cystic Tuft

We imaged with Optos Silverstone platform 11 Cystic Retinal Tufts, that appeared in ultra-wide field color image as round or oval, slightly elevated vitreoretinal degenerations. The lesions appeared small and circumscribed, with a chalky-white color, and vitreous attached to the retinal surface. Ultra-wide field SS-OCT scans revealed hyperreflective irregular elevated lesions with internal hypo reflective cystoid cavities, and normal layers of the neuroepithelium could not be distinguished (Fig 2A, 2B). In all cases peripheral SS-OCT also showed vitreous traction at the apex and vitreous condensation. In 8 cases choroid thinning was appreciable (Fig 2B) and in 5 cases vitreous lacunae were clearly visible (Fig 2C, 2D). In 3 cases full thickness retinal defects were associated (Fig 2D). A posterior vitreous detachment was detected in 2 cases.

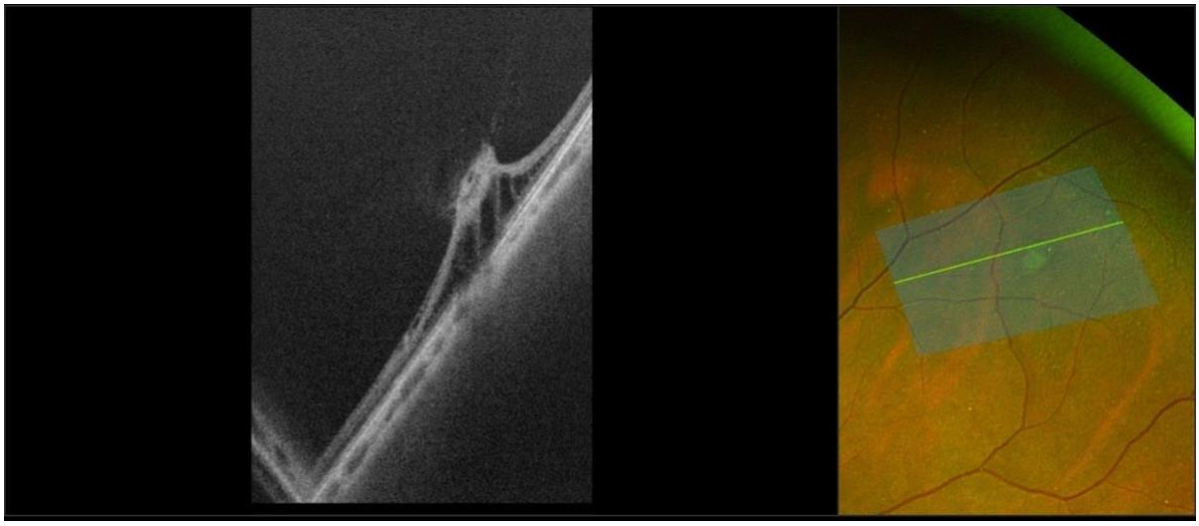

Fig 2A. Cystic tuft. A hyperreflective irregular elevated lesion with internal hypo reflective cystoid cavities is depicted in UWF SS-OCT. Vitreous traction is evident. In color optomap the lesion appears small and circumscribed, with a chalky-white color.

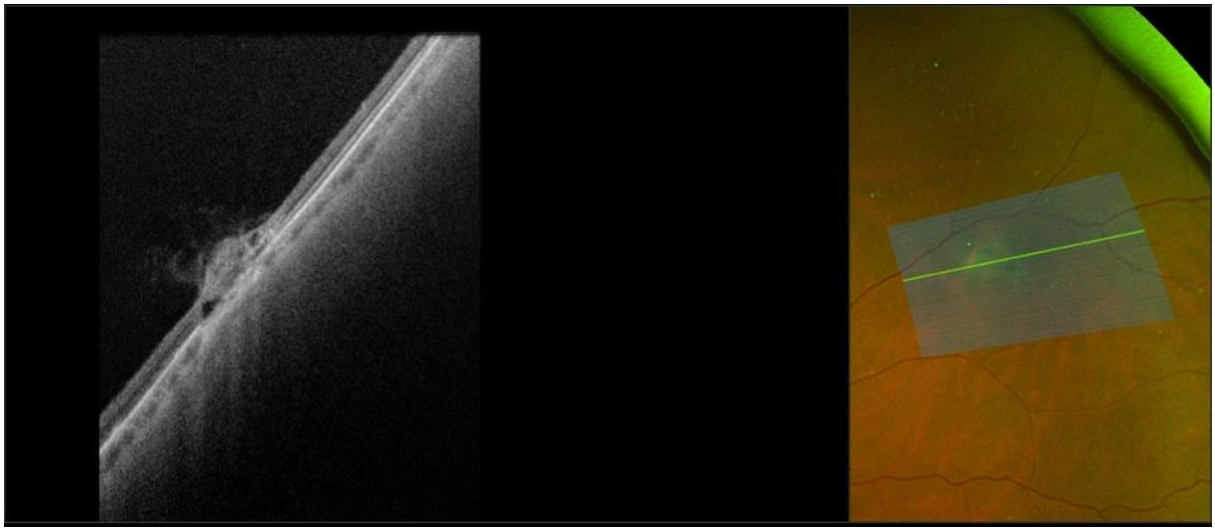

Fig 2B. UWF imaging of tuft. A hyperreflective irregular elevated lesion with some hypo reflective cystoid cavities is depicted in UWF SS-OCT. Normal layers of the neuroepithelium cannot be distinguished, choroidal thinning is appreciable.

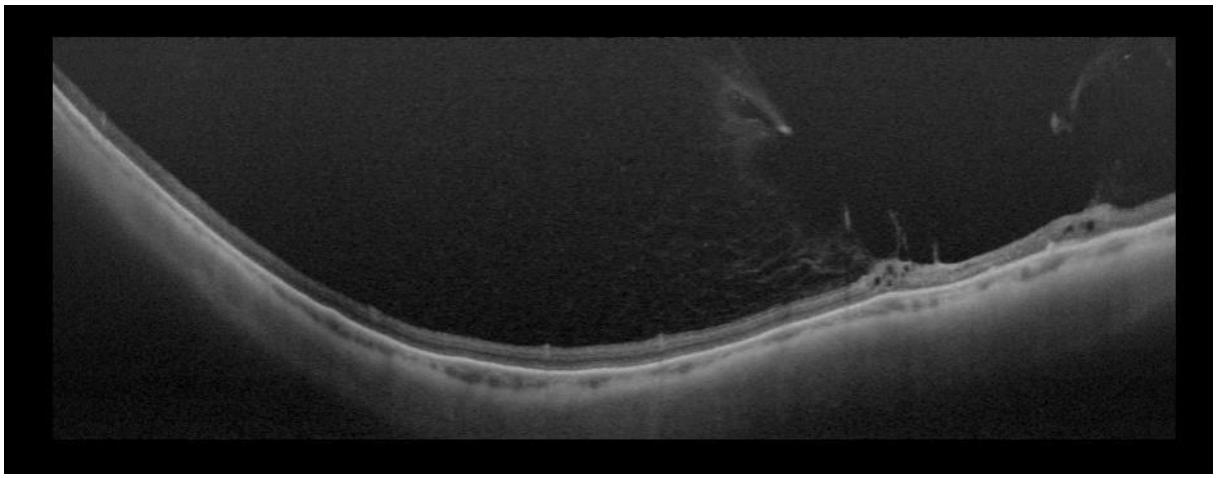

Fig 2C. Cystic tuft on UWF SS-OCT. Vitreous traction, condensed vitreous and a lacuna are clearly visible.

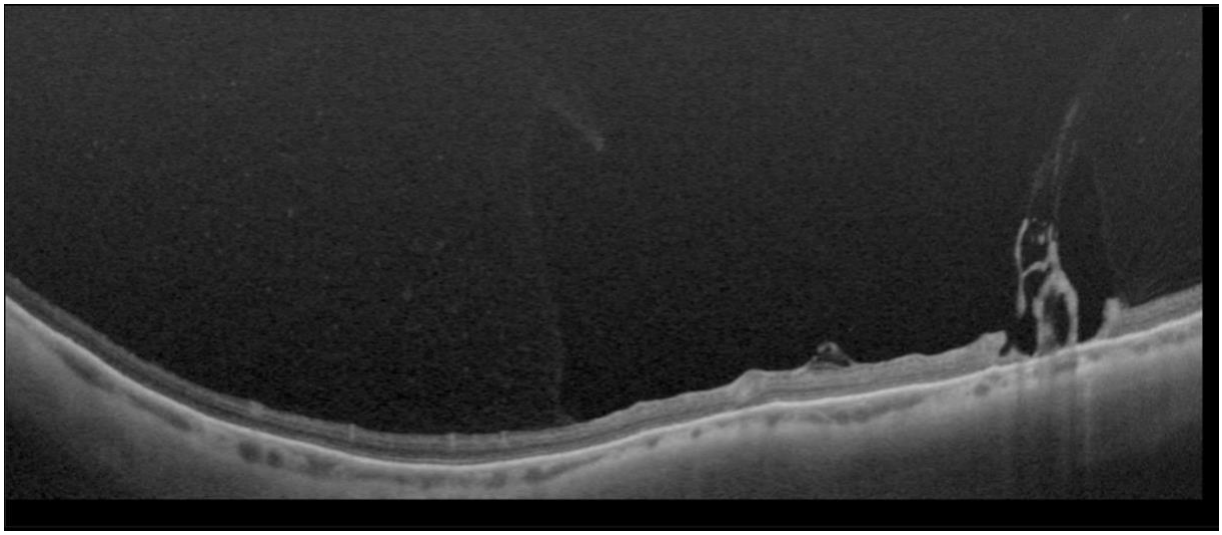

Fig 2D. Cystic tuft on UWF SS-OCT. Vitreous traction, condensed vitreous and a lacuna are clearly visible, full thickness retinal defects are present.

Peripheral Retinal Hole

We analyzed with Optos Silverstone 21 peripheral retinal holes. Peripheral retinal holes appeared in ultra-wide field fundus imaging as round or oval full thickness retinal defects. Ultra-wide field SS-OCT revealed in 15 cases everted edges (Fig. 3D,E,G); while in the other cases the edges were not elevated (Fig. 3B) and in 10 cases an operculum in the nearby vitreous was visible (Fig. 3A). In 9 cases retinal pigmented epithelium appeared irregularly thickened, with irregular deposits (Fig. 3C,D). In 6 cases a circumscribed shallow retinal detachment was associated (Fig. 3D,E). In 9 cases retinal microcystic changes were present (Fig. 3D). In 13 cases vitreous traction at the inner retinal surface was appreciable (Fig. 3D,E), in the others no vitreous traction was appreciable (Fig. 3B,C,F,G). In 9 cases a complete posterior vitreous detachment was present, in 12 cases hyaloid macular detachment was recorded.

In 7 cases the patients reported phosphenes, in 8 cases patients complained about myodesopsya.

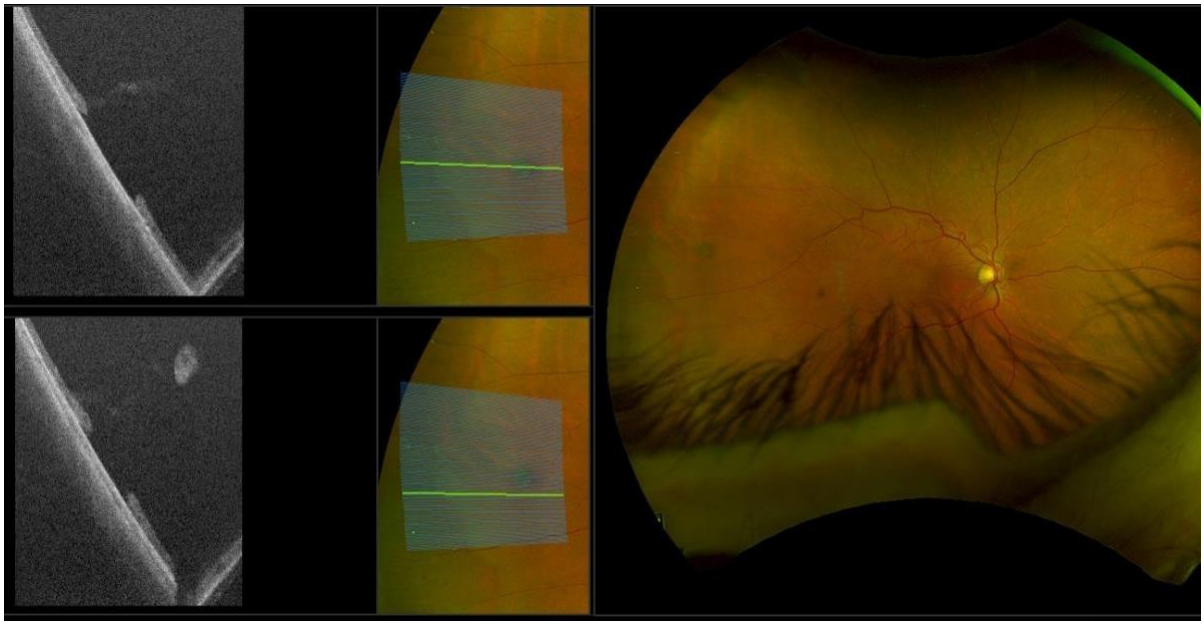

Fig 3A. UWF SS-OCT of peripheral retinal hole, with slightly everted edges, and an operculum in the nearby vitreous. Condensed vitreous at the borders of the hole is visible.

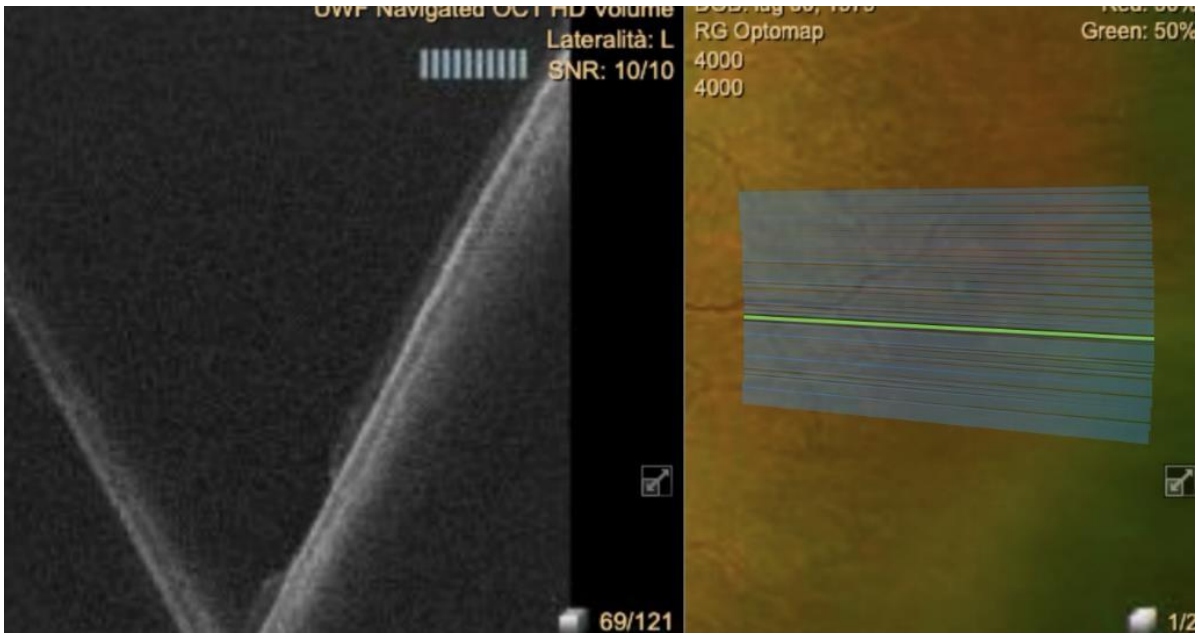

Fig 3B. UWF SS-OCT of peripheral retinal hole, with flat edges, no vitreous traction visible.

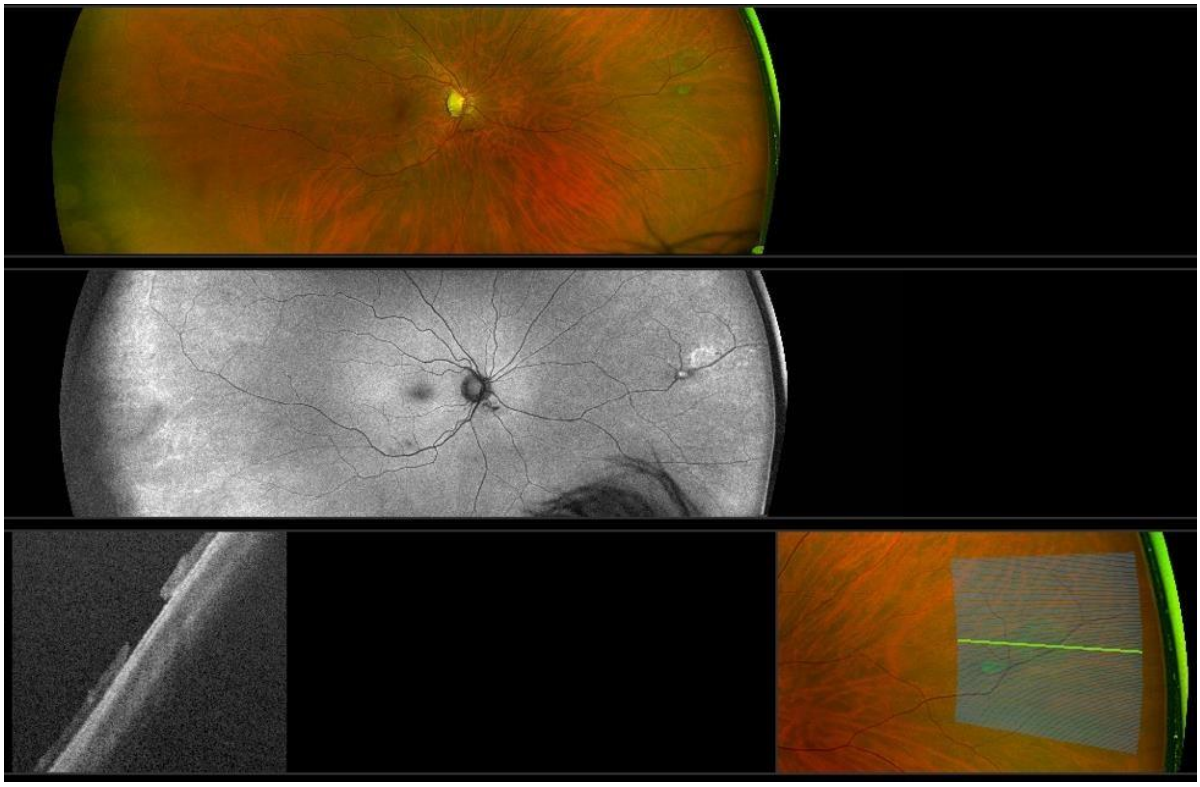

Fig 3C. UWF SS-OCT of peripheral retinal hole. Slightly elevated borders of the hole, intraretinal hyperreflectivity at the border of the hole are appreciable. In color optomap a whitish cuff circumscribing the hole is visible, appearing hyperfluorescent in autofluorescence.

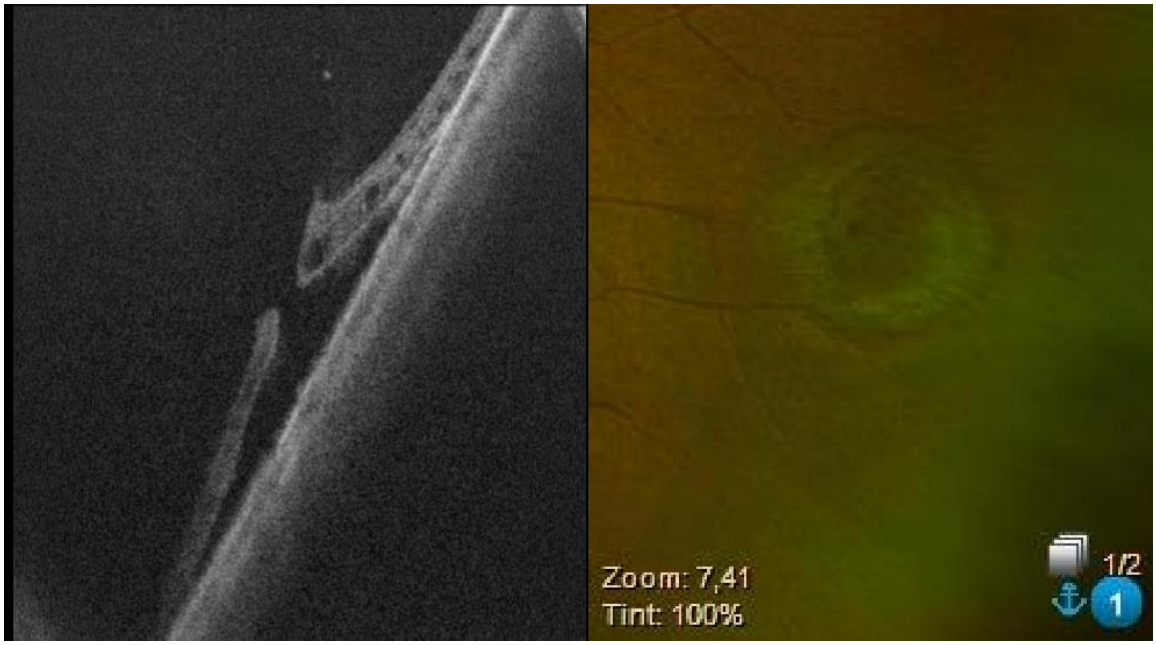

Fig 3D. UWF SS-OCT of peripheral retinal hole with subretinal fluid. Elevated borders of the hole, intraretinal microcystic changes at the border of the hole, irregular retinal pigmented epithelium deposits are appreciable. In color optomap a whitish cuff circumscribing the hole is visible.

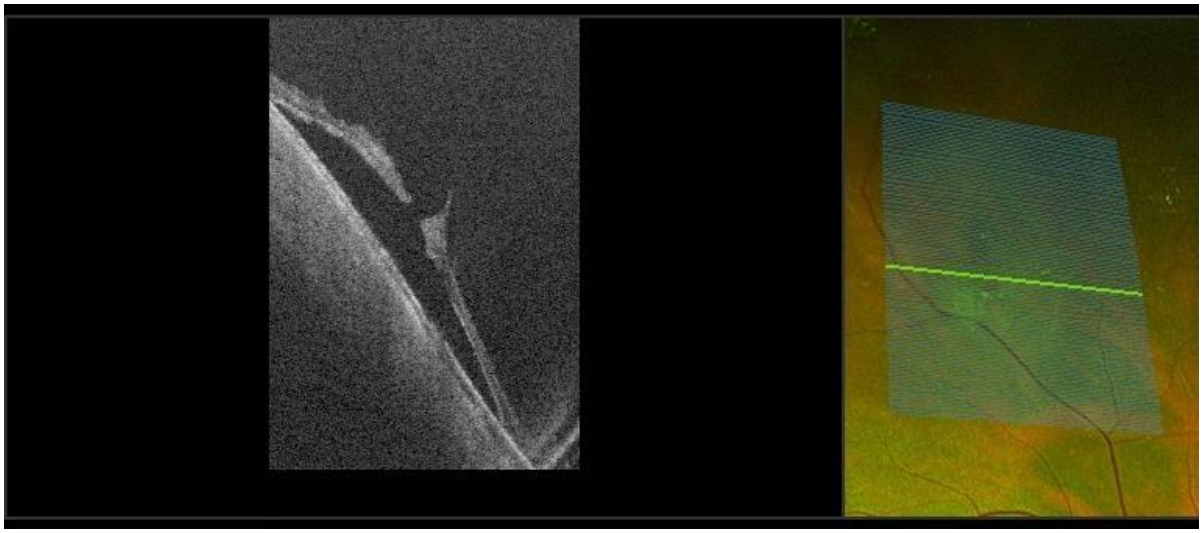

Fig 3E. UWF SS-OCT of peripheral retinal hole with subretinal fluid. Elevated borders of the hole and vitreous traction at the border of the hole are appreciable.

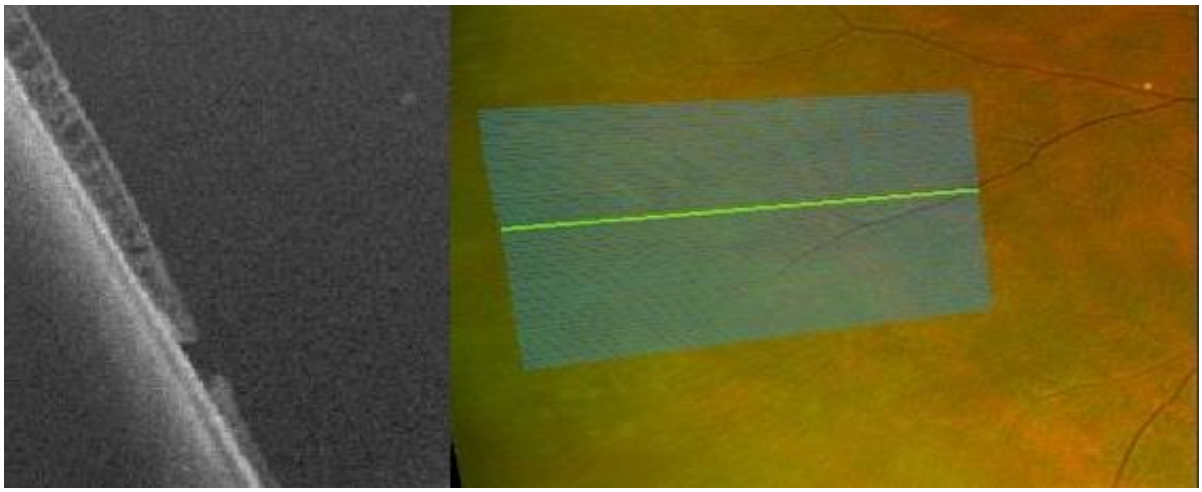

Fig 3F. UWF SS-OCT of peripheral retinal hole, near an area of retinal schisis. Slightly elevated borders of the hole, without subretinal fluid and hyperreflective intravitreal dots are visible.

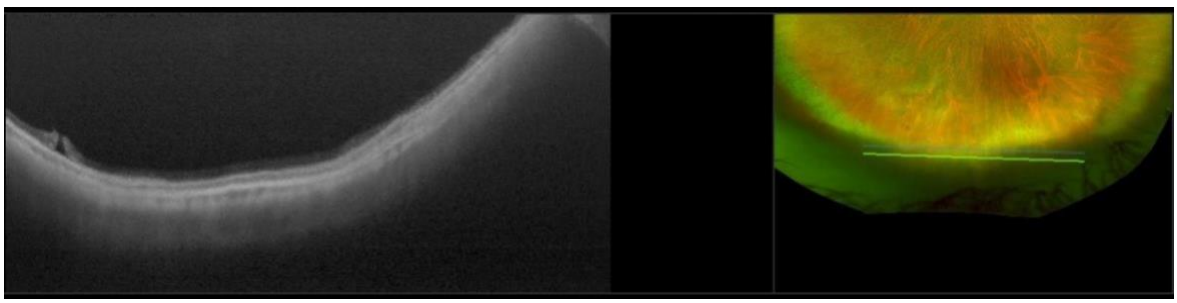

Fig 3G. UWF SS-OCT of peripheral retinal hole. Elevated borders of the hole and intraretinal hyperreflectivity at the border of the hole are appreciable.

Snail track degeneration

We imaged with Optos Silverstone 4 snail track degenerations. In ultra-wide field fundus imaging snail track degeneration appeared as bands of retina composed of tightly spaced white dots, like snowflakes. Irregular thinning and inner retinal hyperreflective dots of the retinal layers were observed in all the lesions on ultra-wide field SS-OCT (Fig. 4). Other OCT findings included diffuse vitreous traction (4 cases), cystoid changes and full thickness holes (2 cases).

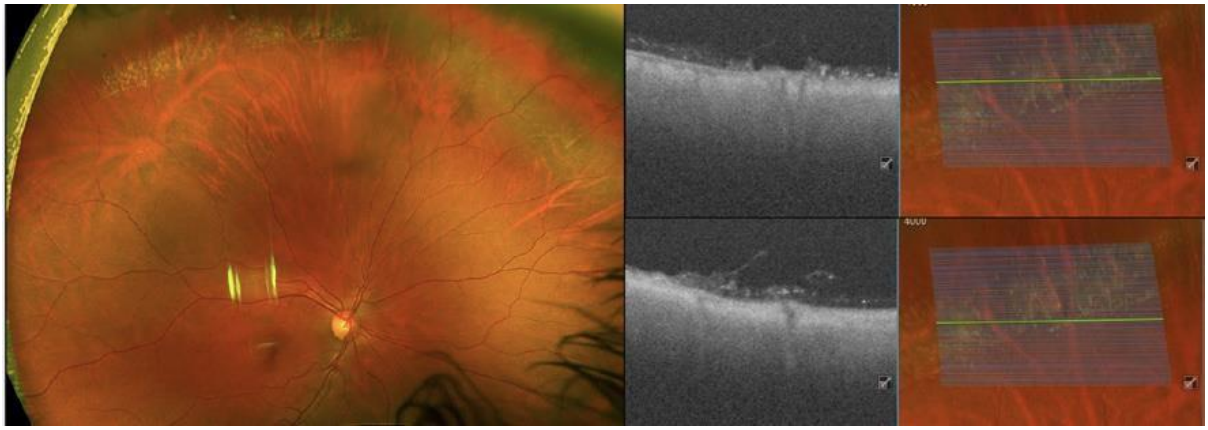

Fig. 4. UWF SS-OCT findings in snail track degeneration. Vitreous traction, irregular retinal thinning, and hyperreflective retinal deposits, with a wrinkled inner retinal surface are showed.

White Without Pressure

In 4 eyes we observed white without pressure degenerations. These lesions appeared in ultra-wide field fundus imaging as irregular, translucent white areas and in peripheral SS-OCT were characterized by hyperreflectivity of the outer retinal layers and ellipsoid zone, without vitreous traction (Fig.5).

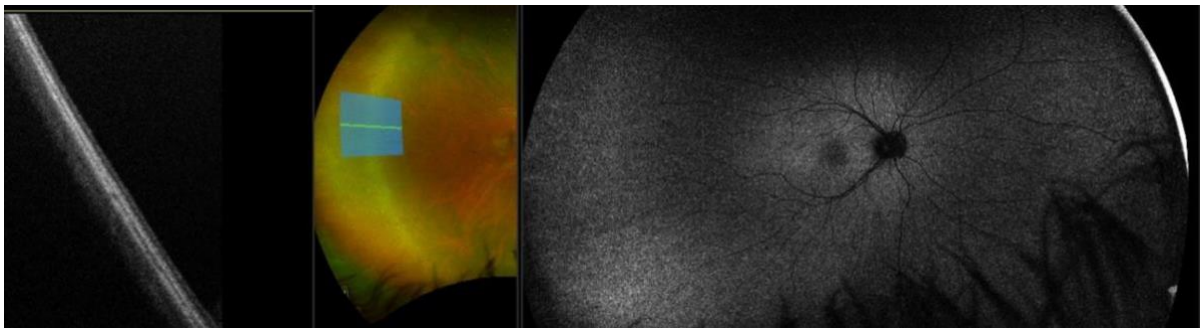

Fig 5. UWF SS-OCT and autofluorescence findings in white without pressure degeneration. This lesion appears in ultra-wide field fundus imaging as an irregular, translucent white area and in peripheral SS-OCT is characterized by hyperreflectivity of outer retinal layers and ellipsoid zone, without vitreous traction. In autofluorescence imaging it shows a slight hyperfluorescence.

Peripheral retinoschisis

We imaged with Optos Silverstone 24 cases of peripheral retinoschisis, in 7 cases a detachment was associated. Peripheral retinoschisis appeared on ultra-wide field fundus imaging as a dome-shaped lesion, with a translucent appearance of the inner retinal surface. In 15 cases inversion artifact of the OCT image, related to an inversion of the image, occurred. Peripheral SS-OCT over the lesions showed a splitting into multiple layers, especially in the inner layers, with a "saw-tooth" schisis-like separation of the retinal layers, intraretinal columns, normal retinal pigmented epithelium (Fig. 6A, 6B, 6C, 6D). In 5 cases, we observed breaks at the level of the external leaflets (Fig 6D, 6E). In some cases, the peripheral SS-OCT clearly showed the edges of the break, firmly adherent to the pigmented epithelium. In some cases, intraretinal hyporeflective cavities dividing the sensorineural retina into inner and outer layers and photoreceptor alterations and disruption were present. The vitreous overlying the lesions in 16 cases was condensed, and in 8 cases vitreoretinal tractions were appreciable.

In 7 cases, SS-OCT showed subretinal fluid, with elevation of the neuroepithelium (schisis-detachment) (Fig. 6F).

In 6 cases a complete posterior vitreous detachment was recorded, in 15 cases posterior vitreous hyaloid was detached. Inversion artifact of the OCT image occurred in 15 cases.

In 2 cases the patients reported phosphenes, in 2 cases patients complained myodesopsya, in most cases were asymptomatic.

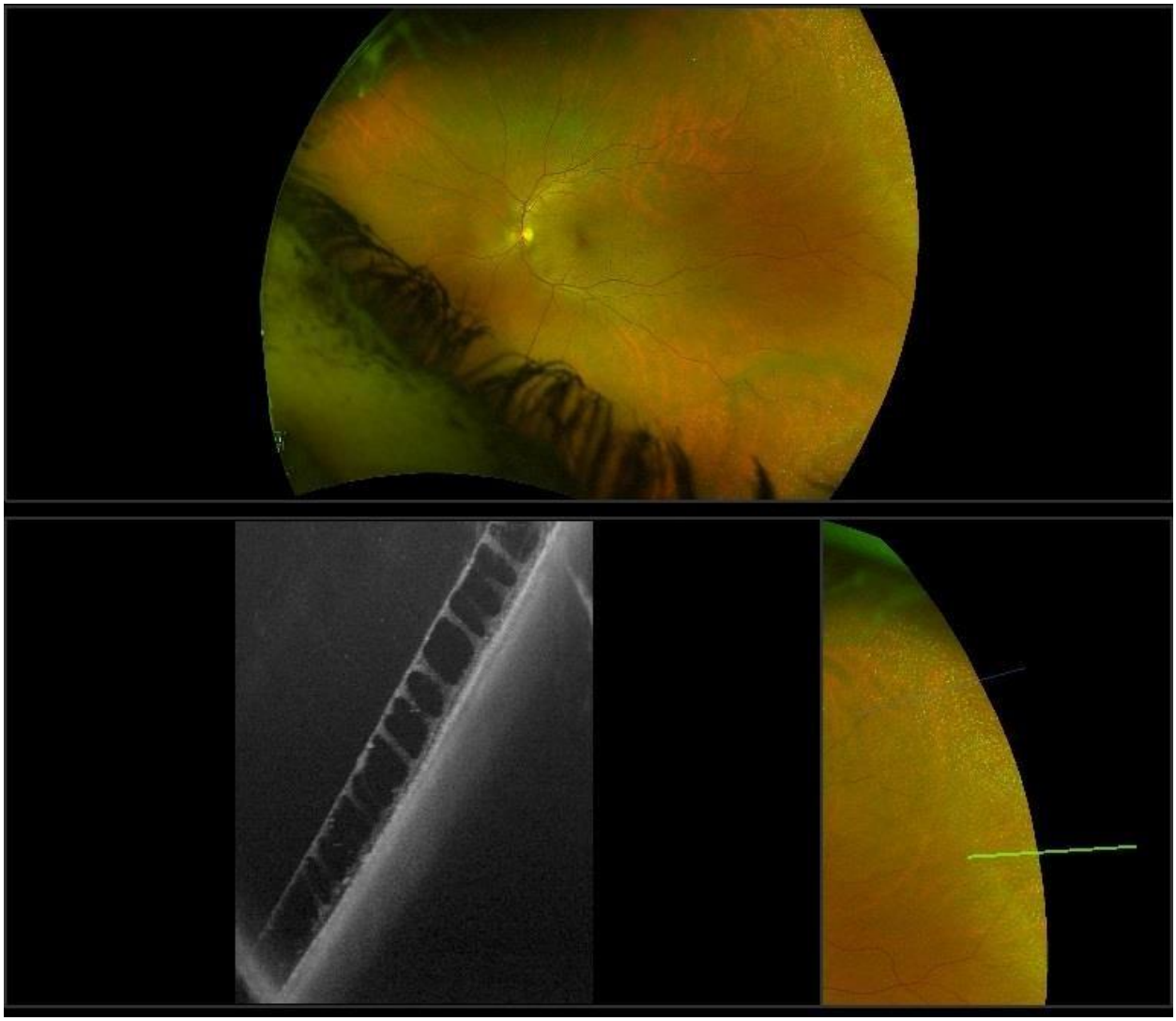

Fig. 6A. In this UWF SS-OCT a typical “saw-tooth” schisis-like separation of the retinal layers, with intraretinal columns, and normal retinal pigmented epithelium is depicted.

Fig. 6B. Peripheral retinoschisis. The lesion appears on UWF fundus imaging as a dome-shaped lesion. UWF SS-OCT shows the typical separation of the retinal layers.

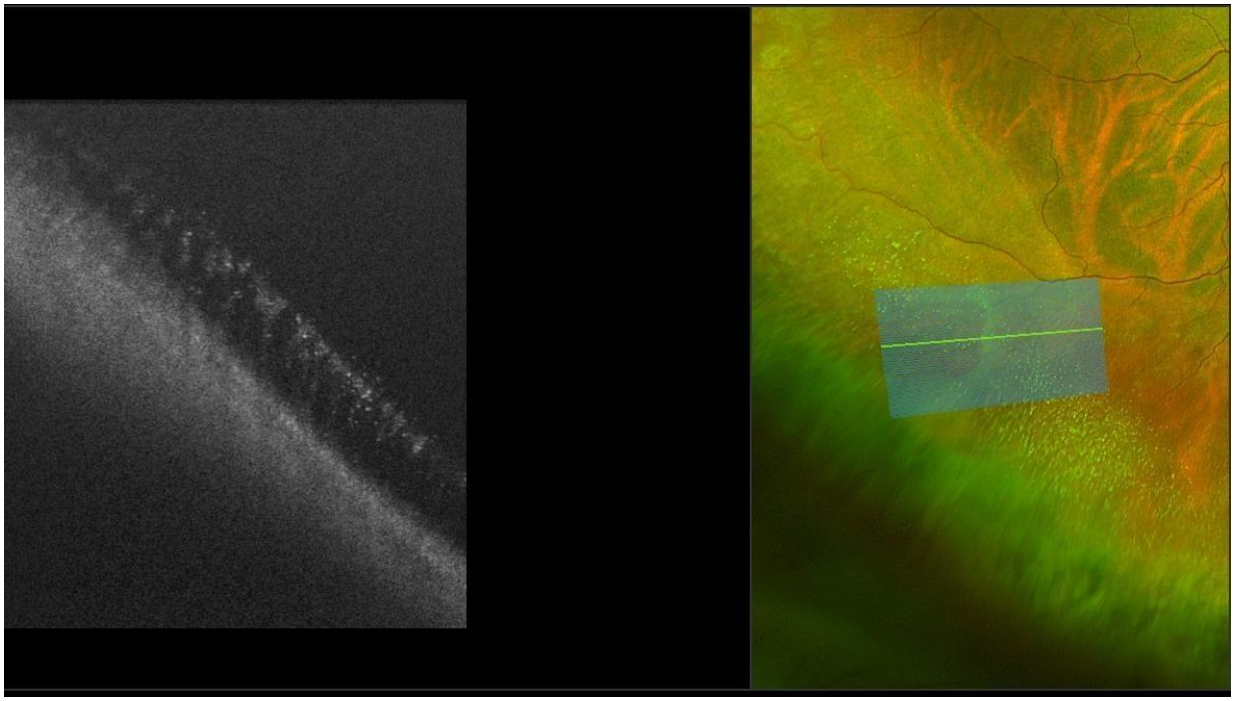

Fig. 6C. Peripheral retinoschisis. The lesion has on UWF optomap a translucent appearance of the inner retinal surface. UWF SS-OCT shows a splitting into multiple layers and intraretinal dots.

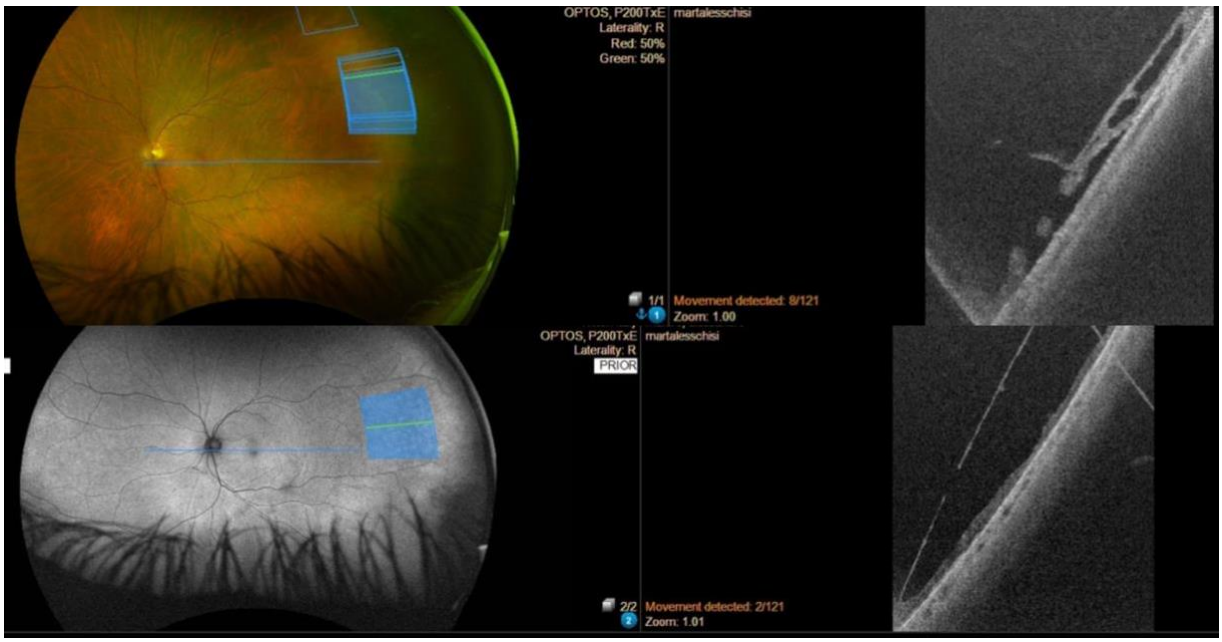

Fig. 6D. Peripheral retinoschisis. UWF SS-OCT shows a splitting into inner retinal layers and external retinal tears. Inverted artifacts are also present.

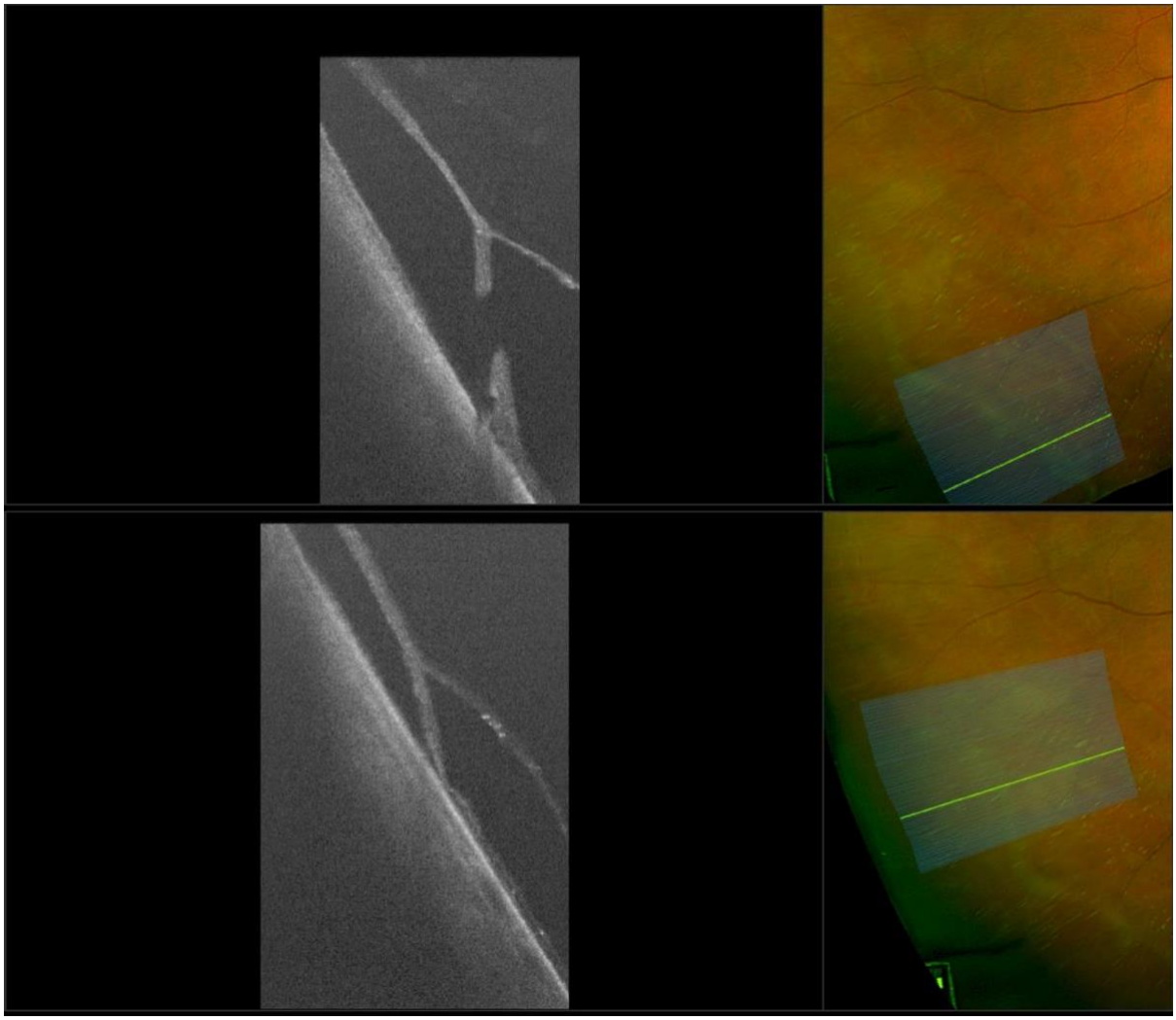

Fig. 6E Peripheral Retinoschisis with external tear. UWF SS-OCT over the lesions clearly shows the edges of the break.

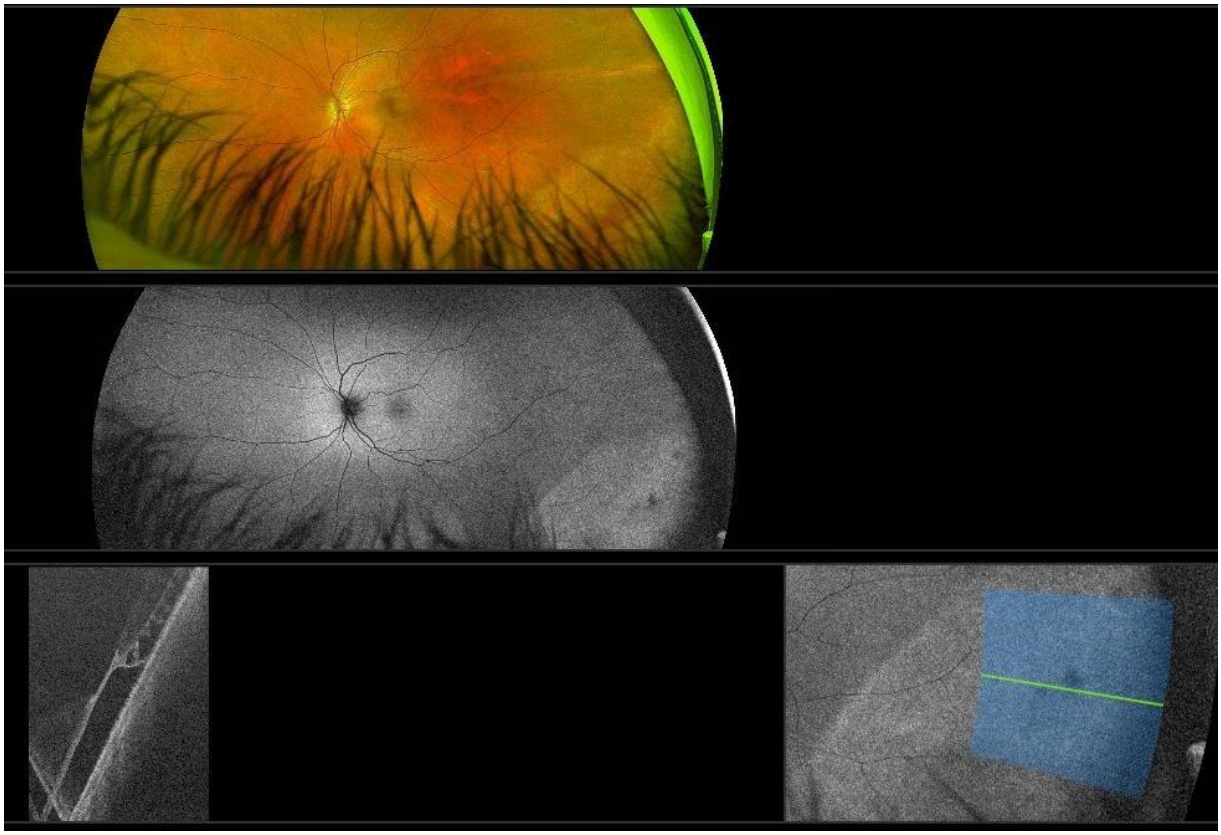

Fig. 6F Peripheral Schisis-Detachment. UWF SS-OCT over the lesions clearly shows a retinal detachment associated to peripheral retinoschisis, not evident in color optomap. In autofluorescence retinal detachment appears slightly more hyperfluorescent than the near area of retinoschisis, but only in UWF SS-OCT the presence of a retinal detachment is evident.

Retinal tear

We analyzed 34 retinal tears, or horseshoe tear, that appeared as full-thickness lesions with a partially detached retinal flap, and vitreous traction (Fig 7A, 7B). Fifteen tears were accompanied by subretinal fluid or subclinical retinal detachment and a partially attached or detached flap (Fig 7A, 7B). In addition, in the eyes with attached flap a hyper-reflectivity of the vitreous adherent to the inner retinal surface could be visualized (Fig 7A, 7B). In 26 retinal tears the imaging was acquired after laser treatment. Retinal pigmented epithelium appeared characterized by a focal hyperreflective thickening in 16 cases (Fig 7B). A posterior vitreous detachment was detected in 25 cases. In 6 cases a various grade of vitreous hemorrhage was associated.

In 14 cases the patients reported phosphenes, in 20 cases patients complained myodesopsya.

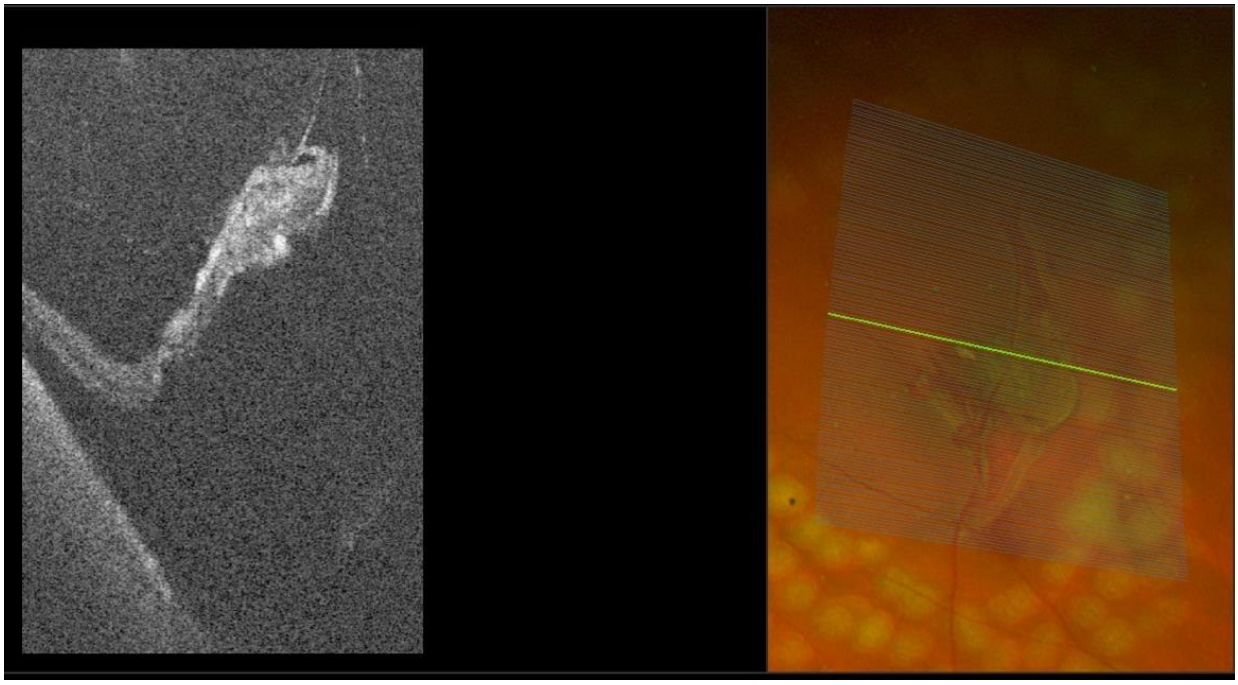

Fig. 7A. UWF SS-OCT on perivascular retinal tear, already treated with laser. OCT shows a shallow retinal detachment, hyperreflectivity on the edge of the tear, and vitreous traction.

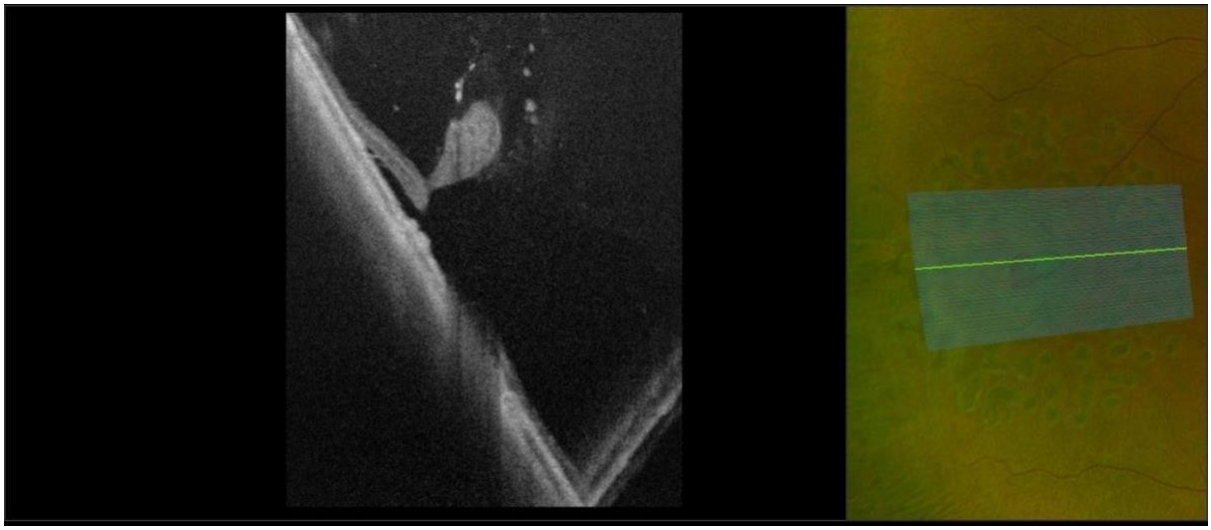

Fig. 7B. UWF SS-OCT on retinal tear, already treated with laser. A shallow retinal detachment, hyperreflectivity on the edge of the tear, vitreous traction, vitreous hyperreflective dots, and irregular thickening of retinal pigmented epithelium are depicted.

Retinal dialysis

We studied 2 cases of retinal dialysis. One case was treated with laser photocoagulation. The retinal dialysis appeared as a circumferential retinal break located at the ora serrata. OCT demonstrated vitreoretinal traction with retinal elevation, rolled edges, and complete absence of the retina more distally, consistent with a dialysis (Fig.8).

Fig. 7B. UWF SS-OCT on retinal dialysis. A shallow retinal detachment, vitreous condensation, enrolled edge of the dialysis are visible. Inverted artifacts are present.

Case series

In the present study we also report a case series of patients in which the ultra-wide field SS-OCT imaging helped the physicians in the diagnosis and supported or changed the clinical decision.

Case 1 – Atrophic peripheral retinal hole

A 60-year-old female patient with a history of central serous chorioretinopathy in her right eye was referred to our emergency department by an external ophthalmologist for potential laser treatment, following the incidental finding of a peripheral retinal hole. The patient was asymptomatic, reporting no phosphenes or floaters, and had been previously diagnosed with a posterior vitreous detachment ten years prior.

Using the Optos Silverstone platform, we examined the retinal periphery and identified an atrophic hole with flat edges and condensed vitreous over the lesion, without any evident vitreous traction. Subretinal fluid was not present. Based on the absence of symptoms and supported by the peripheral OCT findings consistent with an atrophic hole without traction, the physician (DB) decided not to perform laser treatment, hypothesizing that it likely resulted from chronic retinal thinning without rhegmatogenous potential.

Fig 8. UWF Optomap and SS-OCT of a 60-year-old female patient, asymptomatic for phosphenes and myodesopsya. In UWF SS-OCT a peripheral retinal hole, with flat edges, and without vitreous traction is depicted.

Case 2 – Subclinical peripheral retinal hole

A 30-year-old myopic man complaining about rare phosphenes in his left eye presented to our emergency department. Clinical examination of fundus revealed a small, pigmented degeneration in superior-temporal retinal periphery, without frank holes. The patient was referred to our department for ultra-wide field fundus imaging. Ultra-wide field SS-OCT clearly reveled a full thickness retinal hole, with vitreous traction, in the periphery of superior-temporal retina, not clinically detectable. In consideration of the peripheral OCT findings the physician (DB) decided to treat this lesion using laser.

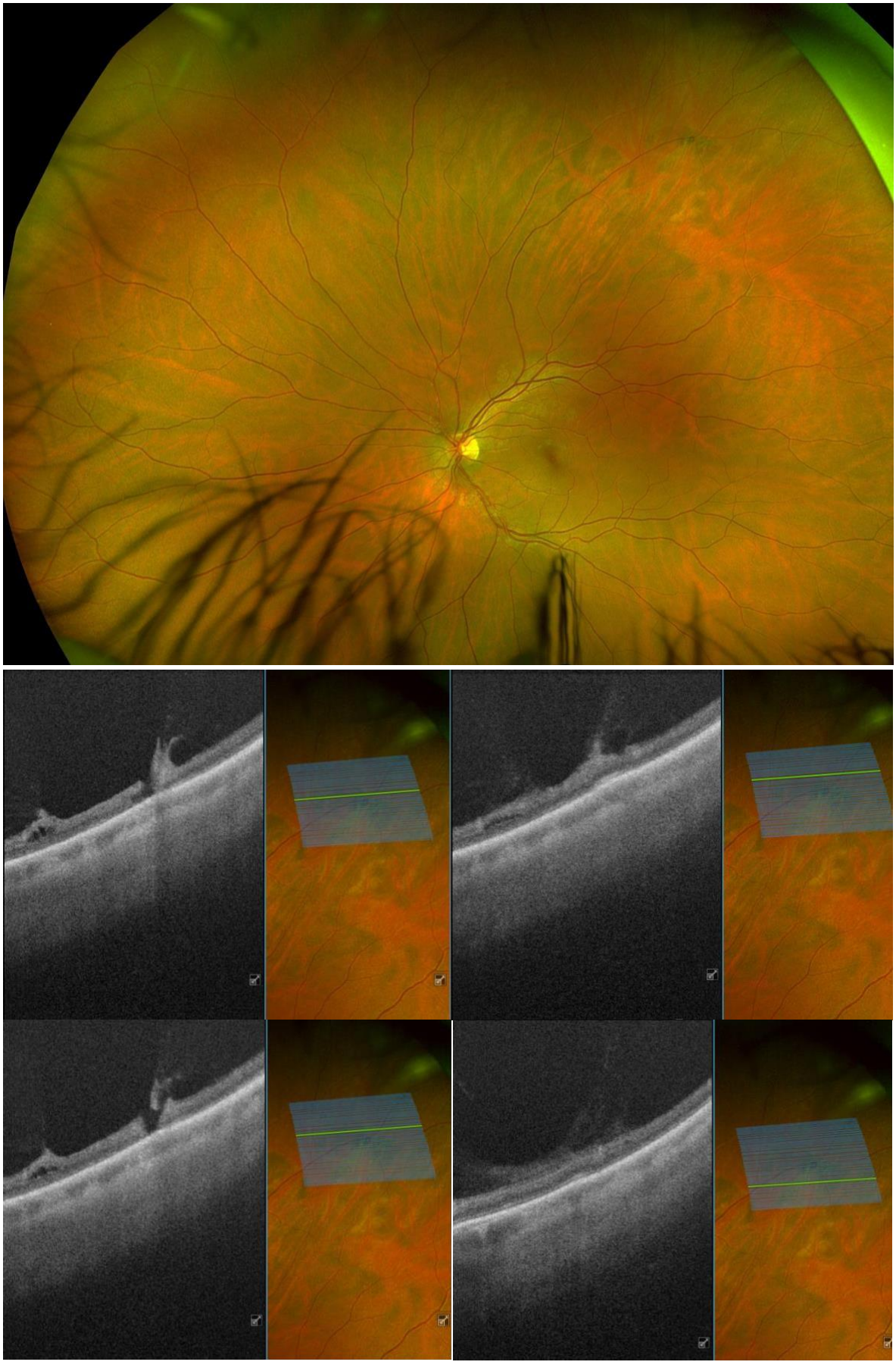

Fig 9. UWF Optomap and SS-OCT of a 30 years-old myopic man, complaining

about rare phosphenes in his left eye. UWF SS-OCT clearly reveals a full thickness retinal hole, with vitreous traction, in the periphery of superior-temporal retina, not clinically detectable.

Case 3 - Cystic tufts

A 24-year-old female patient was referred to our clinic for further evaluation of small, round, slightly elevated vitreoretinal degenerations with a chalky-white appearance, identified in the peripheral retina of both eyes during a routine ophthalmological examination. In the left eye, a hole with an operculum was suspected. The patient was asymptomatic.

We performed a peripheral OCT on the lesions, which revealed the presence of cystic tufts. This imaging was useful for differentiating the lesions from retinal holes and detecting focal vitreoretinal traction over the lesions—subtle features that were not clearly visible on standard ophthalmic examination. Based on the OCT findings, the physician (DB) decided that no treatment was necessary.

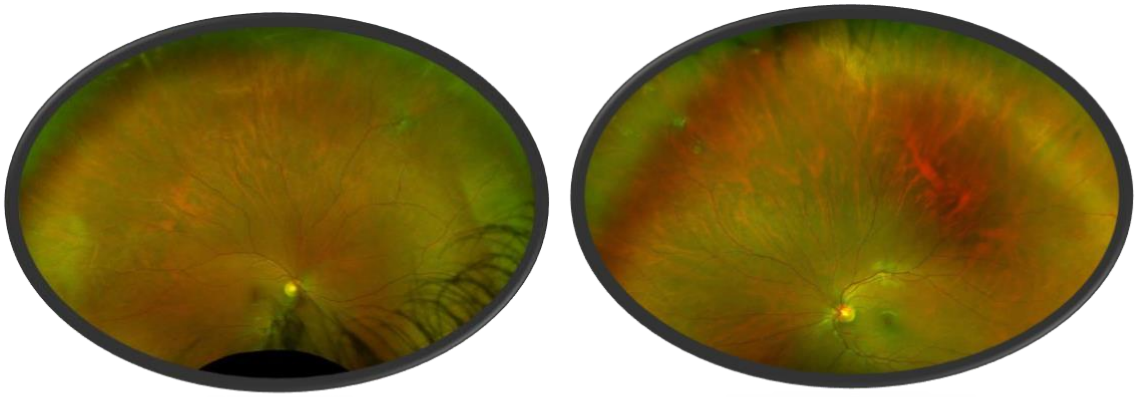

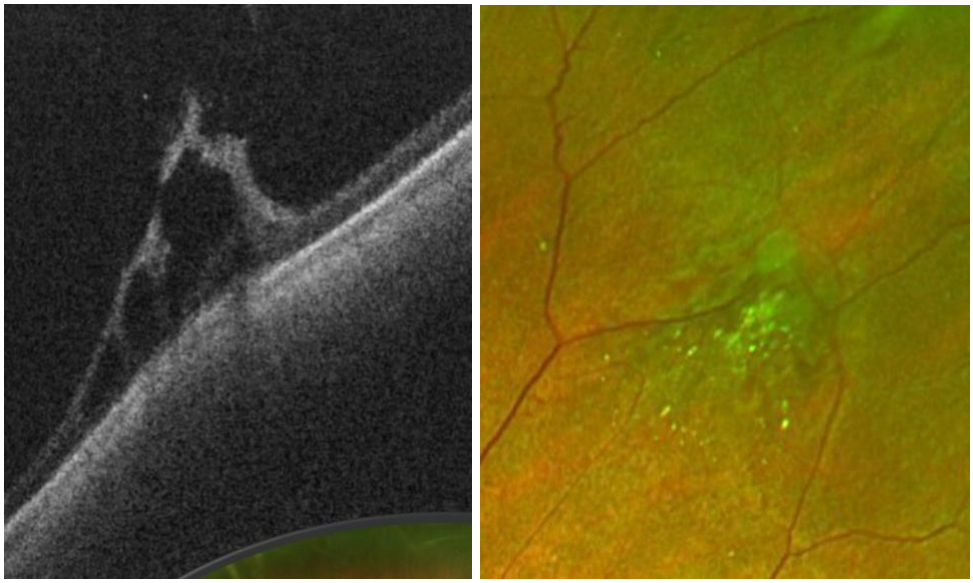

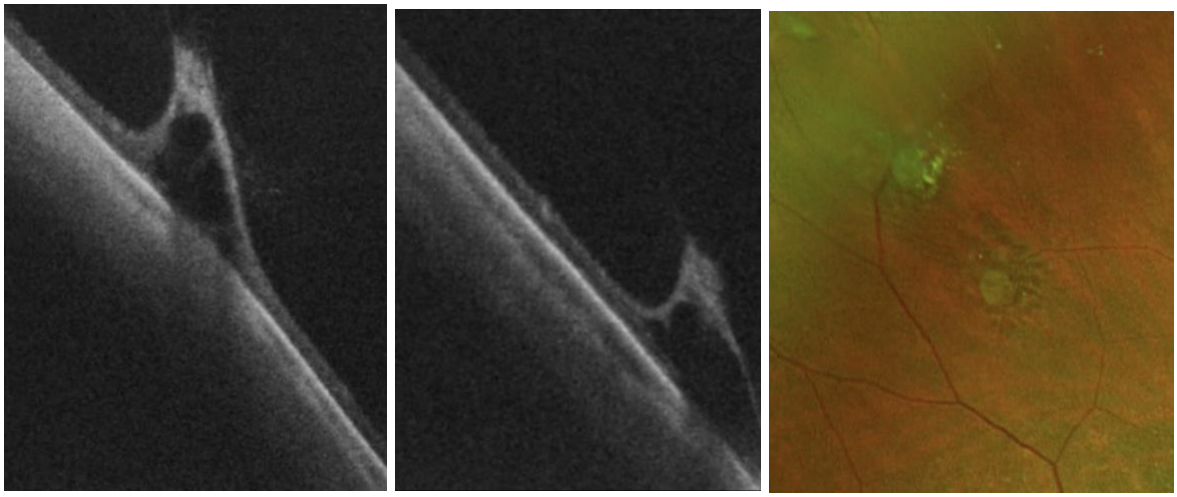

Fig 10. UWF Optomap and SS-OCT of a 24 years-old female patient, asymptomatic for phosphenes and myodesopsya. Small round slightly elevated vitreoretinal degenerations, with a chalky-white color are visible in both eyes. OCT on the lesions reveals the presence of cystic tufts with focal vitreoretinal traction over the lesions. No holes are detected.

Case 4 – Lattice degeneration with vitreous traction

A 52-year-old myopic woman presented with complaints of floaters in her right eye. Fundus examination revealed a posterior vitreous detachment and lattice degeneration. Peripheral OCT was performed, showing marked diffuse vitreous traction over the lesion and a partial-thickness retinal defect. The patient also reported a family history of retinal detachment (father) and had a history of a retinal hole that developed over lattice degeneration in her left eye.

Considering the Optos findings, her symptoms, and the additional risk factors, the physician (DB) decided to treat the lesion with laser.

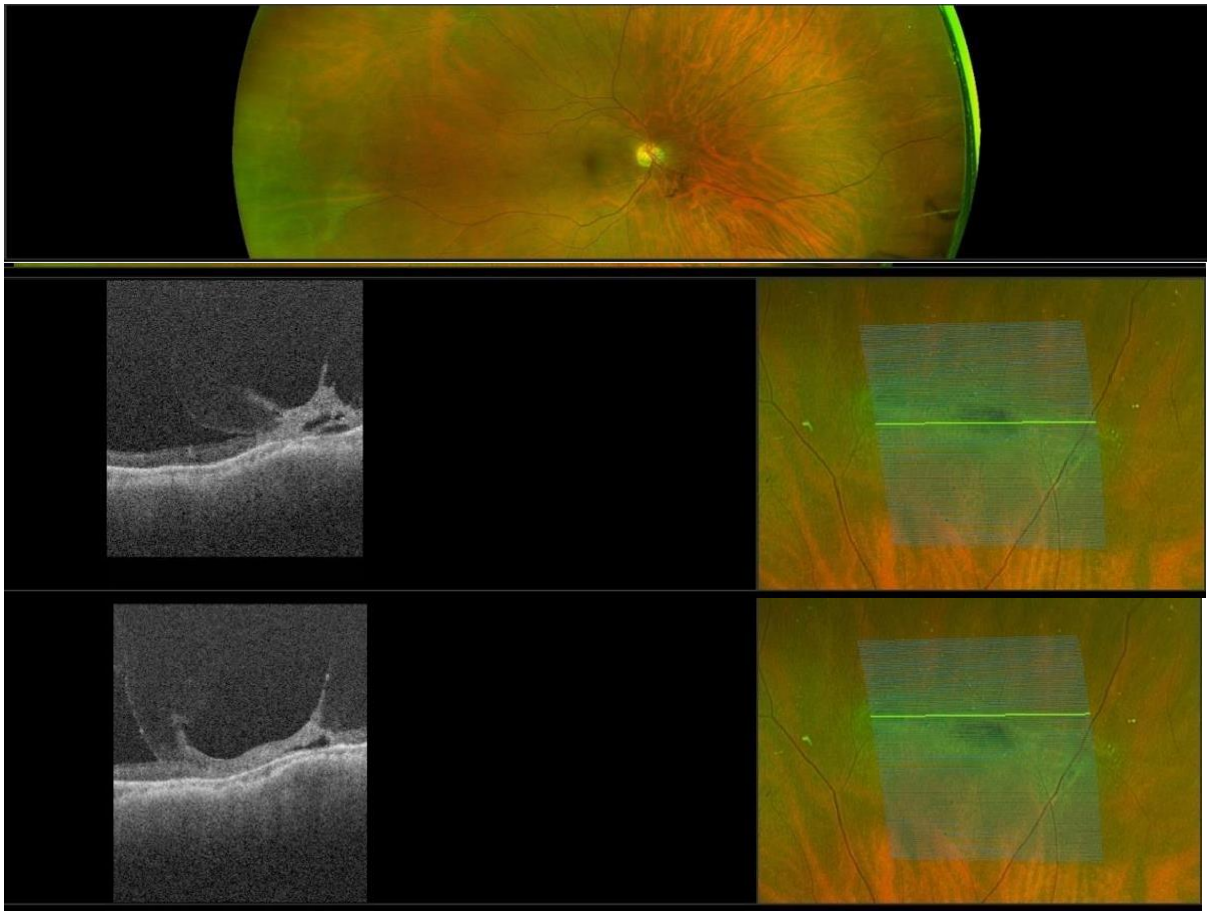

Fig 11. UWF Optomap and SS-OCT of a 52 years-old myopic woman, complaining about myodesopsya in her right eye. In optomap posterior vitreous detachment and a superior lattice degeneration are visible. Peripheral OCT shows diffuse vitreous traction over the lesion, and a partial thickness retinal defect.

Case 5- Schisis/detachment

A 50-year-old female patient during a routinary ophthalmological clinical exam was diagnosed with peripheral retinal schisis in both eyes. The patient did not report phosphenes neither nor myodesopsya. The fundus examination indeed revealed in the left eye a dome shape lesion with a translucent appearance of the inner retinal surface and a demarcation line, in the right eye a translucent appearance of the inner retinal surface was evident. The patient was examined with ultra-wide field OCT that revealed in the left eye a schisis, not associated to a detachment (Fig 11 A) and in the right eye an inferotemporal retinal detachment associated to the schisis (Fig 11 B). The physician (CN) in consideration of OCT findings referred the patient to a vitreoretinal surgeon for surgical evaluation.

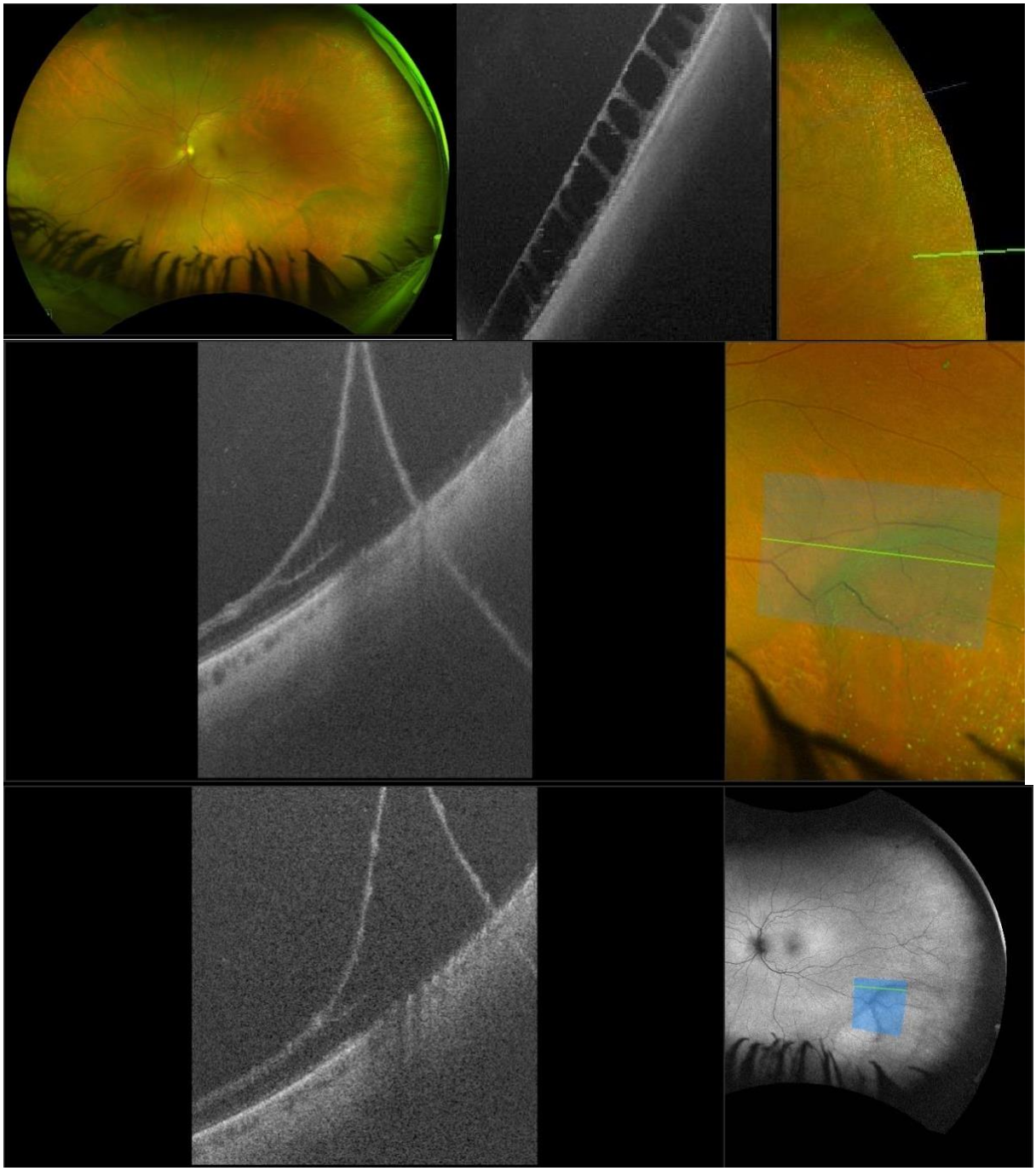

Fig 12 A. UFW Optomap and SS-OCT of left eye, in a 50 years-old woman denying any visual symptoms. Ultra-wide field OCT clearly reveals a schisis in left eye, differentiating it from a retinal detachment. Inverted artifacts are present.

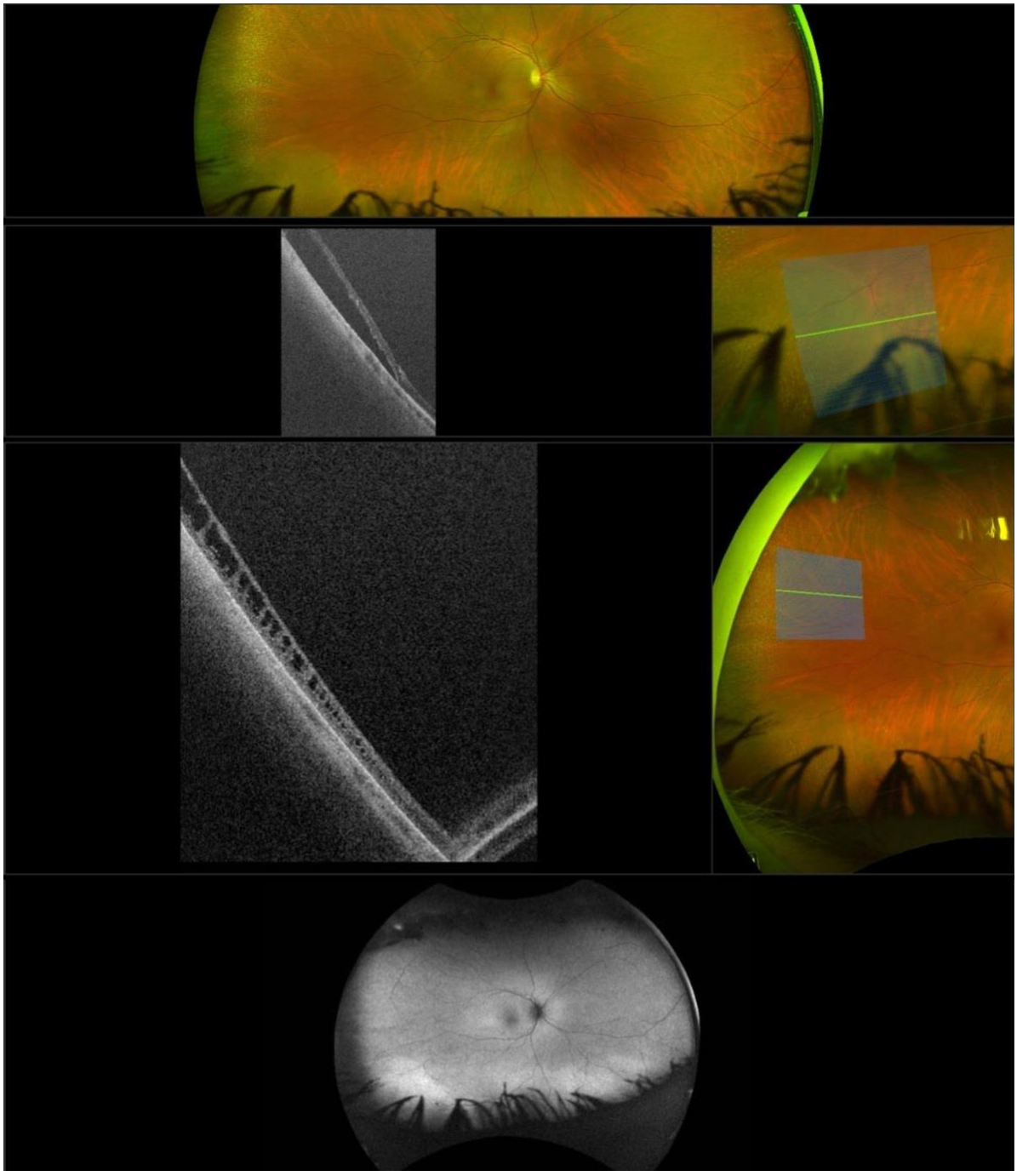

Fig 12 B. Optomap and OCT of right eye, in a 50 years-old woman denying any visual symptoms. Ultra-wide field OCT clearly reveals a schisis, associated to a retinal detachment. The subretinal fluid appears hyperfluorescent in autofluorescence.

Case 6 – Shallow retinal detachment

A 30-year-old female patient underwent surgery for an inferior chronic retinal detachment in her right eye. During follow-up visits, ultra-wide field SS-OCT revealed persistent subclinical subretinal fluid in the operated eye. In her left eye, a slight inferior demarcation line was noted during fundus examination, prompting an Optos imaging assessment. The patient reported no visual symptoms in the left eye.

Ultra-wide field OCT identified a subclinical, shallow retinal detachment in the left eye as well, corresponding to a hyperfluorescent area on ultra-wide field fundus autofluorescence. Based on these findings, the physician (CN) referred the patient to a vitreoretinal surgeon for further surgical evaluation of the left eye.

Fig 13. UWF Optomap and OCT of both eyes, in a 30 years-old woman. In the right eye the patient underwent scleral buckling for chronic retinal detachment. UWF-OCT of the right eye depicted the persistence of subretinal fluid, clearly visible also in autofluorescence image. In the left eye UWF SS-OCT clearly reveals a chronic inferior shallow detachment too, clearly visible also in autofluorescence image.

Discussion

Retinal degenerations are common lesions affecting the peripheral retina, frequently encountered during dilated fundus examination of both symptomatic and asymptomatic patients. Most of these lesions are not significantly associated with an increased risk of rhegmatogenous retinal detachment. However, certain types, such as lattice degeneration, degenerative retinoschisis, retinal tufts, retinal holes, have the potential to lead to rhegmatogenous retinal detachment. The prophylactic treatment of retinal degenerations, through laser or cryotherapy, remains controversial and is not clearly defined by clinical recommendations. As a result, ophthalmologists focus on educating high-risk patients about the signs and symptoms of posterior vitreous detachment and advise them to seek immediate ophthalmological evaluation if these symptoms arise[11,12]. Currently, we rely on the guidelines of the Preferred Practice Pattern from the American Academy of Ophthalmology for the management of these conditions, which primarily consider the presence or absence of symptoms related to posterior vitreous detachment[13]. Current evidence suggests that most peripheral retinal degenerations should not be treated unless in high-risk scenarios, and well-designed, prospective, randomized clinical studies to clarify the benefit-risk ratio of prophylactic treatment are still lacking[11,12].

The evaluation of peripheral retina and vitreoretinal interface plays an important role in screening, diagnosing, monitoring, and treating retinal diseases. Recently, the availability of ultra-wide field high-resolution retinal technologies enabled a better documentation of peripheral retinal lesions, improving their detection and characterization; however, the literature evaluating peripheral retinal degenerations and rhegmatogenous lesions by means of ultra-wide field OCT is still limited.

Thus, we conducted the present study to investigate the feasibility of Optos Silverstone peripheral SS-OCT integrated with a new scanning laser ophthalmoscope ultra-wide-field imaging device to evaluate and better characterize different types of peripheral retinal degenerations and rhegmatogenous lesions.

This multimodal platform integrates ultra-widefield fundus imaging, swept-source SS-OCT, and fundus autofluorescence. Peripheral OCT scanning with Optos Silverstone allows to quickly capture 23-mm line scans in the central retina or smaller line or volume scans in the peripheral retina, not requiring neither image steering nor montaging[14].

In our study, we imaged and provided detailed descriptions of the following peripheral retinal degenerations and rhegmatogenous lesions: lattice degeneration, snail track degeneration, retinal tufts, peripheral retinal holes, retinal tears, peripheral retinoschisis, schisis/detachment, and white without pressure. Volume scans were performed across the areas of interest in all eyes, meticulously examining each scan to identify structural changes present at or adjacent to the peripheral lesions. We will discuss our findings on the most frequently observed peripheral retinal degenerations in detail.

Lattice degeneration

Lattice degeneration is one of the most common and clinically significant peripheral retinal findings, that predisposes to a rhegmatogenous retinal detachment [12,15]. Its prevalence is estimated to be 7–10% of the normal population and up to 42% in myope population, being the most common type[16,17]. In the fellow eyes of patients with retinal detachment, lattice degeneration is present in 9.2% to 35% of patients[18]. Ophthalmoscopically a lattice degeneration appears as a hyperpigmented degenerative lesion with blurred borders and white retinal vessels, with vitreoretinal adhesions and traction. Lattice degenerations appear mostly in the vertical meridian[12]. The pattern of lesions varies. Typically, they appear as multiple concentric lesions, while, in some cases, demonstrate perivascular distribution. Typical distribution appears as a patching pattern within the equatorial area, rarely affecting the central region or the ora serrata[15]. The pathogenesis of this type of lesion is not clear, it has been hypothesized that developmental abnormalities of the internal limiting membrane, dense vitreo-retinal tractions at its margins, and choroidal alterations are involved[19]. Lattice degenerations may be associated to tractional retinal tears following posterior vitreous detachment, due to vitreous traction on the margins of the lesions[12]. The clinical significance of lattice degeneration results from the increased risk of rhegmatogenous retinal detachment in eyes with these lesions. Among several features of lattice degeneration, vitreous adhesion at the borders of the lesion likely plays the most important role followed by retinal thinning, leading to retinal breaks formation[15]. The prevalence of lattice degeneration is in contrast with the annual rate of retinal detachment which does not exceed 0.01–0.02%. However, the cumulation of other risk factors, as myopia, vitreous changes, and intraocular surgery may substantially increase the risk of rhegmatogenous retinal detachment[15].

Our findings on lattice degeneration in our peripheral OCT study are in agreement with the literature [15,19,20]. In our series the most frequent characteristics recorded were thinning of the neurosensory retina, vitreous adhesions, full thickness retinal holes. Also pigmented epithelium deposits were frequently detected, as well as choroid thinning. Specifically peripheral OCT allowed us to observe the morphology of vitreous over the lesion in a greater detail than clinical examination: overlying vitreous liquefaction and firm vitreo retinal adhesions at the edge of the degeneration were a typical finding. The vitreous insertion in lattice degeneration revealed with peripheral OCT was also reported by Govetto et al, who found round, non-operculated holes in retinal lattice with broad vitreous insertion and suggested the hypotheses of tangential traction contributing to the peripheral pathology observed in these lesions[9]. The vitreous insertion in lattice degeneration is consistent with the higher risk of tractional retinal tears following posterior vitreous detachment. OCT findings are in agreement with the histological findings of lattice degenerations, that show the liquefied vitreous over lattice degeneration, adherent vitreous at the margins of the degenerated area, a discontinuous internal limiting membrane and atrophic inner retinal layers. The histological findings also show that lattice degeneration is predominantly associated with lipid inclusions and intraretinal fibrils

in glial cells[21]. Some authors also reported that migration, proliferation, and differentiation of retinal pigmented epithelium cells might be involved in the development of retinal lattice degeneration, demonstrated by means of histological studies[22].

Cystic Retinal Tufts

Cystic Retinal Tufts are developmental vitreoretinal abnormalities in which retina is stretched by the overlying vitreous cortex and persistent vitreous traction may lead to retinal tears and detachment. They are clinically characterized by round or oval, slightly elevated vitreoretinal degenerations, small and circumscribed, with a chalky-white color. Vitreous condensations are attached to tuft surface, and the lesion may have pigmentary changes at the base. The cystic retinal tuft occurs most frequently in the extra basal or equatorial zone of the eye[23]. It seems to be a congenital abnormality in the development of the peripheral retina and affects approximately 5% of the population. The risk of developing a rhegmatogenous retinal detachment from a cystic retinal tuft is reported to be 0.28%, and prophylactic treatment is not indicated. However, these lesions have a risk of progression toward vision-threatening retinal detachment because they may be avulsed by vitreous traction, resulting in a full-thickness retinal break. Retinal tears at tufts regions may be responsible for as many as 10% of clinical retinal detachments associated with posterior vitreous detachment[24].

We imaged with Optos Silverstone 11 Cystic Retinal Tufts. Ultra-wide field fundus imaging allowed us to see retinal tufts in detail, by navigating over the lesion. In all cases peripheral SS-OCT showed vitreous traction at its apex due to condensed vitreous. The lesions appeared on OCT as hyperreflective irregular elevated lesions with internal hyporeflective cystoid cavities, and normal layers of the neuroepithelium could not be distinguished. These results are in agreement with another report on ultra-wide field imaging on retinal tufts and are similar to the characteristic intralesional cystic changes on histopathological analysis of these degenerations [25].

Histologically, the cystic retinal tufts are characterized by a dome-shaped area with internal microcysts, accumulations of glial tissue form in nodules on the retinal surface that enclose crypts of formed vitreous within the lesion. Large tufts demonstrate outer retinal degeneration, and photoreceptor loss. The dense vitreoretinal adhesion in cystic retinal tufts may explain this common association with retinal tears that can have either a flap or an operculum and can occur with or without a posterior vitreous detachment[24].

Therefore, prophylactic laser treatment should be considered for such cases of cystic retinal tufts with retinal tears and follow-up for those without such signs[25].

The utility of peripheral OCT imaging in characterization of retinal tufts is the differentiation from retinal holes, the detection of focal vitreoretinal traction over the lesion, and of progression to a full-thickness retinal break, due to the avulsion of

the traction, subtle features that are often not evident on standard ophthalmic examinations.

Peripheral retinal holes

Holes of the peripheral retina are full thickness retinal defects, usually smaller than tears. Retinal holes are usually slowly progressive and shallow, as they are a result of atrophic changes in the neurosensory retina; while operculated holes are the result of vitreous traction. Prophylactic laser treatment is frequently performed in operculated holes and is usually not performed for atrophic retinal holes[18].

We analyzed with Optos Silverstone 21 peripheral retinal holes. Peripheral retinal holes appeared in wide field fundus imaging as round or oval full thickness retinal defects. We found that peripheral SS-OCT imaging was particularly useful for the identification of potential rhegmatogenous characteristics associated to retinal holes, as vitreoretinal traction, everted edges or subretinal fluid, not always clinically evident on fundus examination.

In our series we observed 2 different SS-OCT patterns: in one type everted edges, subretinal fluid, cystoid changes in the surrounding retina, and vitreous adhesion at the inner retinal surface were more frequently present, and sometimes an operculum was observed floating in the nearby vitreous; in the other one localized retinal thinning, with flat edges and sometimes cystoid changes in the surrounding retina, without vitreous adhesion or subretinal fluid were observed.

We may define the first type, characterized by focal vitreoretinal traction, that sometimes results in operculated holes as not atrophic hole. Conversely, we may define the second type as atrophic, as we hypothesize that it is a result of a progressive localized retinal thinning and probably carry a lower risk of retinal detachment.

Similarly, Choudry et al described retinal holes with an inverted V-shaped profile (operculated holes), with the presence of vitreous adhesion to the retinal surface and a complete or partial attachment of the operculum; and holes with a flat-shaped profile, that did not show any vitreous adhesion or subretinal fluid[5].

Also, Govetto et al in an imaging study on rhegmatogenous retinal lesions and peripheral vitreo-retinal interface with wide-field OCT, distinguished operculated and non-operculated holes, hypothesizing that the pathogenesis of operculated holes was similar to horseshoe tears, involving a posterior vitreous detachment in all cases. Moreover, the authors reported signs of peripheral vitreo-retinal tractions over non operculated holes and found that they were more often associated with retinal detachment. Nevertheless, the authors found a high prevalence of vitreoschisis associated to non-operculated peripheral retinal holes, hypothesizing that these lesions are the result of a vitreous traction mainly tangential to the retina and that they should not be considered atrophic[9,26].

Snail track degeneration

Snail track degeneration is characterized by demarcated bands of glistening, closely packed white frost-like appearance lesions, often oval or elongated, resembling a track left by a snail. Snail-track degeneration, as well as lattice degeneration, is characterized by retinal thinning with vitreous liquefaction above the lesion, but marked vitreous traction is rarely present, although round holes are common. Snail track degeneration is usually found closer to the equator and parallel to the ora serrata, and it tends to uniformly distribute evenly between the four quadrants. The prevalence of snail-track degeneration in general population is 10 %, it affects myopic eyes more frequently (40 %)[27]. This kind of lesions has not been associated with an increased risk of retinal breaks or retinal detachment[26,27,28,29,30]. It has been hypothesized by some to represent a precursor on mild form of lattice degeneration[26]. Snail-track degeneration is often complicated by retinal holes, less frequently by flap tears with traction[18].

In our imaging study, we imaged with Optos Silverstone 4 snail track degeneration, that appeared on color optomap as bands of retina composed of tightly - spaced white dots, similar to snowflakes. Ultra-wide field SS-OCT depicted a retinal thinning and an irregular and wrinkled inner retinal surface, without marked condensations or tractions of the overlying vitreous, and sometimes atrophic retinal holes, corresponding to multiple dark irregular areas. It also showed intraretinal deposits. These findings are in agreement with other reports and with histological studies, that show the association of snail track degeneration with organelle degeneration within retinal neurons[18]. Histology also suggests no involvement of the vitreoretinal interface in snail-track degeneration[21].

When snail track degenerations are associated with multiple atrophic holes and full-thickness retinal tears, these characteristics may be appreciated in ultra-wide field OCT more easily than with ophthalmoscopic examination, helping the clinician to identify the lesions with higher rhegmatogenous risk.

White Without Pressure

White without pressure can be considered an optical phenomenon in retinal periphery characterized by the fundus color change from orange-red to translucent white, without a mechanical stimulus. Lesions are usually located beyond the equator, although changes may occur near the major retinal vascular arcades[31].

It is most common in young myopic patients. Retinal breaks, including giant tears, occasionally develop along the posterior border of this kind of retinal degenerations, although it has not been significantly associated with vitreoretinal tractions and retinal breaks, so this degeneration is not considered an indication for prophylactic laser photocoagulation. The patient should be routinely examined every 1–2 years, informed about the symptoms of a retinal tear or detachment and asked to have retinal examination if these symptoms occur. Other experts consider it a trophic-tractional phenomenon, or vitreoretinal degeneration with the risk of linear and giant retinal tears along the posterior margin of the lesion[18,32].

In our study we imaged with Optos Silverstone 4 lesions. On color optomap white without pressure presented as irregular, translucent areas and in peripheral SS-OCT corresponded to hyperreflective outer retinal layers and ellipsoid zone, without any signs of vitreo-retinal traction. These findings are in agreement with previous reports[32,33], in which white without pressure was shown not to have relation to vitreo-retinal traction, but to the reflectivity changes in the photoreceptor layer, which is consistent with our study.

Peripheral retinoschisis

Degenerative retinoschisis consists in the splitting of the neuro-retinal layers, starting from the peripheral retina and involving the external plexiform layer[34,35]. Acquired retinoschisis has a prevalence of 1.6-7% of the general population and is more frequent after the fourth decade of life. Senile retinoschisis can be associated with retinal detachment in 2.5–10.5% of cases but is the primary cause in only 0.05–2.5% of the total[18].

As far as management is concerned, in most cases it can be monitored, but in symptomatic cases or cases with progression, especially towards the posterior pole, or if the development of a retinal detachment occurs, it may require intervention, however there are no definitive guidelines for management[36].

Histopathological studies suggest that it develops from the confluence of peripheral microcystic degeneration, due to elongation of supporting glial cells, and rupture of Muller cells, with the appearance of superficial cavities separating the retina; however, the etiology is not fully understood[37].

Clinically, acquired peripheral retinoschisis has a dome-shaped appearance, most often it is bilateral, and is localized in the inferotemporal retinal periphery, with a translucent appearance of the inner retinal surface[34,35]. When associated with rhegmatogenous retinal detachment, the retinal surface is more typically wrinkled, with the presence of breaks in both the outer and inner layers or full-thickness retinal breaks[35]. Detachments starting from a cleft consist of a retinoschisis cavity with a rupture of the outer wall, with the presence of subretinal fluid and it is sometimes difficult to differentiate a cleft from a retinal detachment by clinical examination. Chronic retinal detachments may also occasionally mimic a cleft due to their atrophic appearance.

We imaged with Optos Silverstone 24 cases of peripheral retinoschisis, in 7 cases a detachment was associated. We observed on SS-OCT a typical splitting into multiple layers, especially in the inner layers, with a “saw-tooth” schisis-like separation of the retinal layers, intraretinal columns, normal retinal pigmented epithelium. Intraretinal hyporeflective cavities dividing the neuroretina into inner and outer layers could be observed, we may hypothesize that they correspond to Müller cells elongated to separate the cavities. In some cases, we observed breaks at the level of the external leaflets. In 7 cases OCT showed neuroretina detachment and subretinal fluid (schisis-detachment). The differentiation of retinoschisis from retinal detachment can be difficult to understand with an indirect ophthalmoscope alone. In our series

the use of peripheral OCT was useful for the confirmation of the diagnosis of peripheral retinoschisis, for the identification of tears in its leaflets and for the identification of associated retinal detachment, similarly to other authors[38,39], even if the inversion artifact of the OCT image, related to an inversion of the image, occurred in the imaging of 15 cases.

Retinal tears

A peripheral retinal break, or horseshoe tear, is as a full-thickness retinal lesion with a partially detached retinal flap, and vitreous traction. Isolated tears are considered the most severe retinal degeneration because of a high risk of rhegmatogenous retinal detachment (2.9–18 %)[40]. The prevalence of isolated retinal tears is 9–12 % in general population[18]. Flap tears with vitreous traction are associated with retinal detachment in 33–55 % of cases[23]. Retinal tears are caused by traction at the sites of vitreoretinal adhesion that often occurs in acute posterior vitreous detachment. Retinal tears are reported to occur in eyes with posterior vitreous detachment in 8.2–47.6 % of cases[18].The frequency of flap tears in idiopathic intraocular hemorrhage and in posterior vitreous detachment was reported to be 70 % and 15 %, respectively. Prophylactic laser treatment is indicated in all cases of retinal dialysis and flap tears[18]. Symptomatic retinal tears with persistent vitreous traction are an indication for immediate prophylactic treatment[23].

We analyzed with Optos Silverstone 34 retinal flap tears; in 26 cases the imaging was acquired after laser treatment. In 25 cases a complete posterior vitreous detachment was present. In 6 cases a various grade of vitreous hemorrhage was associated. Fifteen tears were accompanied by subretinal fluid or subclinical retinal detachment and a partially attached or detached flap. In addition, in the eyes with attached flap a hyper-reflectivity of the vitreous adherent to the inner retinal surface could be visualized. Vitreous traction could not always be seen during ophthalmoscopy or in color optomap, but was clearly appreciable in SS-OCT. A frequent finding was focal hyperreflective thickening of retinal pigmented epithelium.

General considerations

The primary aim of the present study was to analyze ultra-wide field SS-OCT scans and color optomap images of peripheral retinal degenerations and rhegmatogenous retinal lesions, acquired using the Optos Silverstone device. We sought to examine the structural alterations in the retina associated with these lesions and the vitreo-retinal interface at and around the lesions. In our study we described ultra-wide field OCT findings associated to different retinal degeneration and rhegmatogenous lesions, carrying out a systematic evaluation of full-thickness alterations, subretinal fluid, vitreoretinal traction, and other relevant characteristics. Ultra-wide field SS-OCT provided high-quality and clinically meaningful images of the peripheral neuroretina and vitreoretinal interface. Additionally, we reported a series of cases in which peripheral OCT was particularly valuable in identifying features that

influenced clinical decisions. We described how the peripheral SS-OCT findings contributed to final clinical decisions, guiding the physician toward treatment rather than observation, or vice versa. Nevertheless, these considerations are subjective, and further studies are required to determine if and how peripheral imaging may impact management decisions in clinical practice. The legal implications of such studies are significant, particularly when peripheral lesions are referred for laser treatment but do not exhibit rhegmatogenous characteristics. The assessment of these lesions using ultra-wide field OCT provides valuable documentation that supports clinical decision-making. This detailed evaluation can help substantiate the rationale behind opting for observation rather than intervention. Proper documentation of the imaging findings reinforces the clinician decision-making process and highlights the importance of thorough investigation in cases whit high suspect of peripheral lesions.

This study has several limitations: its retrospective design, the limited number of eyes analyzed, and the cross-sectional nature of the study without a proper follow up. An evaluation over time of specific structural characteristics, such as increased vitreous traction or changes in the amount of associated peripheral subretinal fluid, may assist ophthalmologists in determining when and if intervention is necessary[5]. Further prospective comprehensive studies, which proper follow up are required to evaluate which specific OCT findings may correlate with a higher risk of rhegmatogenous retinal detachment.

Conclusion

In the present study we assessed peripheral retinal degenerations and rhegmatogenous lesions using ultra-wide field SS-OCT integrated with a new scanning laser ophthalmoscope ultrawide-field imaging device, to evaluate and better characterize different types of retinal degenerations.
In our experience, this new OCT technology and scanning technique provided high-quality and clinically meaningful images of the peripheral retina and vitreoretinal interface, adding useful details regarding the ultrastructure of retinal peripheral degenerations, as the presence of subretinal fluid, full thickness retinal defects, or vitreous traction. The characterization of peripheral retinal degeneration with ultrawide field SS-OCT contributed to enhance our understanding of such lesions. In some cases, ultra-wide field OCT imaging facilitated the detection of subtle features of peripheral retinal lesions hidden during standard ophthalmological exam. We hypothesize that the detailed characterization of retinal degenerations may help clinicians to better evaluate the rhegmatogenous risk associated with these lesions and may provide potential advantages in clinical practice, supporting management decisions, especially in doubtful lesions. However, further comprehensive studies are required to analyze which characteristics of retinal degenerations relate to a higher rhegmatogenous risk and to explore whether peripheral SS-OCT evaluation can provide insights that directly influence management decisions.

References

1. Huang D, Swanson EA, Lin CP, et al. Optical coherence tomography. *Science*. 1991;254(5035):1178-1181. doi:10.1126/SCIENCE.1957169
2. Fujimoto J, Swanson E. The Development, Commercialization, and Impact of Optical Coherence Tomography. *Invest Ophthalmol Vis Sci*. 2016;57(9):OCT1-OCT13. doi:10.1167/IOVS.16-19963
3. Nagiel A, Lalane RA, Sadda SR, Schwartz SD. ULTRA-WIDEFIELD FUNDUS IMAGING: A Review of Clinical Applications and Future Trends. *Retina*. 2016;36(4):660-678. doi:10.1097/IAE.0000000000000937
4. Choudhry N, Duker JS, Freund KB, et al. Classification and Guidelines for Widefield Imaging: Recommendations from the International Widefield Imaging Study Group. *Ophthalmol Retina*. 2019;3(10):843-849. doi:10.1016/J.ORET.2019.05.007
5. Choudhry N, Golding J, Manry MW, Rao RC. Ultra-Widefield Steering-Based Spectral-Domain Optical Coherence Tomography Imaging of the Retinal Periphery. *Ophthalmology*. 2016;123(6):1368-1374. doi:10.1016/J.OPHTHA.2016.01.045
6. Fan W, Wang K, Ghasemi Falavarjani K, et al. Distribution of Nonperfusion Area on Ultra-widefield Fluorescein Angiography in Eyes With Diabetic Macular Edema: DAVE Study. *Am J Ophthalmol*. 2017;180:110-116. doi:10.1016/J.AJO.2017.05.024
7. Nadelmann JB, Gupta MP, Kiss S, et al. Ultra-Widefield Autofluorescence Imaging of Retinal Detachment Compared to Retinoschisis. *Ophthalmic Surg Lasers Imaging Retina*. 2019;50(9):550-556. doi:10.3928/23258160-20190905-03
8. Kumar V, Surve A, Kumawat D, et al. Ultra-wide field retinal imaging: A wider clinical perspective. *Indian J Ophthalmol*. 2021;69(4):824-835. doi:10.4103/IJO.IJO_1403_20
9. Govetto A, Sebag J, Lucchini S, et al. IMAGING RHEGMATOGENOUS RETINAL LESIONS AND PERIPHERAL VITREORETINAL INTERFACE WITH WIDEFIELD OPTICAL COHERENCE TOMOGRAPHY. *Retina*. 2024;44(2):269-279. doi:10.1097/IAE.0000000000003946
10. Kovacs KD, Mahrous MA, Gonzalez L, et al. Feasibility and Clinical Utility of Ultra-Widefield-Navigated Swept-Source Optical Coherence Tomography Imaging. *J Vitreoretin Dis*. 2021;5(5):396-404. doi:10.1177/2474126421997335
11. Flaxel CJ, Adelman RA, Bailey ST, et al. Posterior Vitreous Detachment, Retinal Breaks, and Lattice Degeneration Preferred Practice Pattern®. *Ophthalmology*. 2020;127(1):P223-P258. doi:10.1016/J.OPHTHA.2019.09.027
12. Lewis H. Peripheral retinal degenerations and the risk of retinal detachment. *Am J Ophthalmol*. 2003;136(1):155-160. doi:10.1016/S0002-9394(03)00144-2
13. Posterior Vitreous Detachment, Retinal Breaks, and Lattice Degeneration PPP 2019 - American Academy of Ophthalmology. Accessed November 3, 2024. https://www.aao.org/education/preferred-practice-pattern/posterior-vitreous-detachment-retinal-breaks-lattice
14. Sodhi SK, Golding J, Trimboli C, Choudhry N. Feasibility of peripheral OCT imaging using a novel integrated SLO ultra-widefield imaging swept-source OCT device. *Int Ophthalmol*. 2021;41(8):2805-2815. doi:10.1007/S10792-021-01837-7
15. Maltsev DS, Kulikov AN, Shaimova VA, Burnasheva MA, Vasiliev AS. Spotlight on Lattice Degeneration Imaging Techniques. *Clin Ophthalmol*. 2023;17:2383-2395. doi:10.2147/OPTH.S405200
16. Byer NE. Lattice degeneration of the retina. *Surv Ophthalmol*. 1979;23(4):213-248. doi:10.1016/0039-6257(79)90048-1

17. Manjunath V, Taha M, Fujimoto JG, Duker JS. Posterior lattice degeneration characterized by spectral domain optical coherence tomography. *Retina*. 2011;31(3):492-496. doi:10.1097/IAE.0B013E3181ED8DC9
18. Shaimova VA. Peripheral retinal degenerations: Optical coherence tomography and retinal laser coagulation. *Peripheral Retinal Degenerations: Optical Coherence Tomography and Retinal Laser Coagulation*. Published online May 2, 2017:1-227. doi:10.1007/978-3-319-48995-7/COVER
19. Tsai CY, Hung KC, Wang SW, Chen MS, Ho TC. Spectral-domain optical coherence tomography of peripheral lattice degeneration of myopic eyes before and after laser photocoagulation. *J Formos Med Assoc*. 2019;118(3):679-685. doi:10.1016/J.JFMA.2018.08.005
20. Kurobe R, Hirano Y, Ogura S, Yasukawa T, Ogura Y. Ultra-Widefield Swept-Source Optical Coherence Tomography Findings of Peripheral Retinal Degenerations and Breaks. *Clin Ophthalmol*. 2021;15:4739-4745. doi:10.2147/OPTH.S350080
21. Bec P, Malecaze F, Arne JL, Mathis A. [Lattice degeneration of the peripheral retina: ultrastructural study]. *Ophthalmologica*. 1985;191(2):107-113. doi:10.1159/000309568
22. Mizuno H, Fukumoto M, Sato T, et al. Involvement of the Retinal Pigment Epithelium in the Development of Retinal Lattice Degeneration. *Int J Mol Sci*. 2020;21(19):1-11. doi:10.3390/IJMS21197347
23. Brinton DA., Wilkinson CP., Hilton GF. Retinal detachment : principles and practice. Published online 2009:258.
24. Byer NE. Cystic retinal tufts and their relationship to retinal detachment. *Arch Ophthalmol*. 1981;99(10):1788-1790. doi:10.1001/ARCHOPHT.1981.03930020662007
25. Li H, Chen L, Wu M, Zheng B. Spectral-domain optical coherence tomography characteristics of cystic retinal tuft. *BMC Ophthalmol*. 2022;22(1). doi:10.1186/S12886-022-02636-Z
26. Shukla M, Ahuja OP. A possible relationship between lattice and snail track degenerations of the retina. *Am J Ophthalmol*. 1981;92(4):482-485. doi:10.1016/0002-9394(81)90639-5
27. Conart JB, Baron D, Berrod JP. [Degenerative lesions of the peripheral retina]. *J Fr Ophtalmol*. 2014;37(1):73-80. doi:10.1016/J.JFO.2013.09.001
28. Hyams SW, Neumann E. Peripheral retina in myopia. With particular reference to retinal breaks. *Br J Ophthalmol*. 1969;53(5):300-306. doi:10.1136/BJO.53.5.300
29. Kottow M. Peripheral retinal degenerations and breaks. *Albrecht Von Graefes Arch Klin Exp Ophthalmol*. 1980;214(1):53-60. doi:10.1007/BF00414537
30. Hyams SW, Neumann E, Friedman Z. Myopia-aphakia. II. Vitreous and peripheral retina. *Br J Ophthalmol*. 1975;59(9):483-485. doi:10.1136/BJO.59.9.483
31. Karlin DB, Curtin BJ. Peripheral chorioretinal lesions and axial length of the myopic eye. *Am J Ophthalmol*. 1976;81(5):625-635. doi:10.1016/0002-9394(76)90129-X
32. Diaz RI, Sigler EJ, Randolph JC, Rafieetary MR, Calzada JI. Spectral domain optical coherence tomography characteristics of white-without-pressure. *Retina*. 2014;34(5):1020-1021. doi:10.1097/IAE.0000000000000012
33. Yu H, Luo H, Zhang X, Sun J, Zhong Z, Sun X. Analysis of White and Dark without Pressure in a Young Myopic Group Based on Ultra-Wide Swept-Source Optical Coherence Tomography Angiography. *J Clin Med*. 2022;11(16). doi:10.3390/JCM11164830

34. Byer NE. Long-term natural history study of senile retinoschisis with implications for management. *Ophthalmology*. 1986;93(9):1127-1137. doi:10.1016/S0161-6420(86)33601-7
35. Byer NE. Perspectives on the management of the complications of senile retinoschisis. *Eye (Lond)*. 2002;16(4):359-364. doi:10.1038/SJ.EYE.6700191
36. Hoerauf H, Joachimmeyer E, Laqua H. Senile schisis detachment with posterior outer layer breaks. *Retina*. 2001;21(6):602-612. doi:10.1097/00006982-200112000-00007
37. BR S, RY F. Typical and reticular degenerative retinoschisis. *Am J Ophthalmol*. 1973;75(4):123-130. doi:10.1016/0002-9394(73)90809-X
38. Jalalizadeh RA, Smith BT. Characterization and diagnosis of retinoschisis and schisis detachments using spectral domain optical coherence tomography. *Graefes Arch Clin Exp Ophthalmol*. 2023;261(2):375-380. doi:10.1007/S00417-022-05801-8
39. Ho VY, Wehmeier JM, Shah GK. WIDE-FIELD INFRARED IMAGING: A Descriptive Review of Characteristics of Retinoschisis, Retinal Detachment, and Schisis Detachments. *Retina*. 2016;36(8):1439-1445. doi:10.1097/IAE.0000000000000963
40. Robertson DM, Norton EWD. Long-term follow-up of treated retinal breaks. *Am J Ophthalmol*. 1973;75(3):395-404. doi:10.1016/0002-9394(73)91148-3